Acta Crystallographica Section B
Structural Science
ISSN 0108-7681

Chiral *versus* racemic building blocks in supramolecular chemistry: tartrate salts of organic diamines

Dorcas M. M. Farrell,[a] George Ferguson,[a,b] Alan J. Lough[c] and Christopher Glidewell[a]*

[a]School of Chemistry, University of St Andrews, St Andrews, Fife KY16 9ST, Scotland, [b]Department of Chemistry and Biochemistry, University of Guelph, Guelph, Ontario, Canada N1G 2W1, and [c]Lash Miller Chemical Laboratories, University of Toronto, Toronto, Ontario, Canada M5S 3H6

Correspondence e-mail: cg@st-andrews.ac.uk

Received 17 October 2001
Accepted 15 November 2001

In the 1:1 adducts $C_{12}H_{10}N_2\cdot C_4H_6O_6$ formed between 1,2-bis(4′-pyridyl)ethene and racemic tartaric acid [(I), triclinic $P\bar{1}$, $Z' = 1$] and (2*R*,3*R*)-tartaric acid [(II), triclinic $P1$, $Z' = 2$], the ionic components are linked by hard hydrogen bonds into single sheets, which are further linked by C—H···O hydrogen bonds. In the analogous adducts $C_{10}H_{18}N_2\cdot C_4H_6O_6$ formed by 4,4′-bipyridyl with racemic tartaric acid [(III), triclinic $P\bar{1}$, $Z' = 1$] and the chiral acid [(IV), monoclinic $P2_1$, $Z' = 1$], the hard hydrogen bonds generate bilayers which are again linked by C—H···O hydrogen bonds. Piperazine forms a 1:1 salt $[\{(C_4H_{10}N_2)H_2\}^{2+}]\cdot[(C_4H_4O_6)^{2-}]$ with (2*R*,3*R*)-tartaric acid [(V), monoclinic $P2_1$] sheets, which are linked by the cations to form a pillared-layer framework. In each of the 1:2 salts formed by racemic tartaric acid with piperazine [(VI), monoclinic $P2_1/n$, $Z' = 0.5$] and 1,4-diazabicyclo[2.2.2]octane (DABCO) [(VII), monoclinic $P2_1/n$, $Z' = 0.5$], the cation lies across a centre of inversion, with the $[\{HN(CH_2CH_2)_3NH\}^{2+}]$ cation disordered over two sets of sites: in both (VI) and (VII) the anions form a three-dimensional framework encapsulating large voids which accommodate the cations. The salt formed between DABCO and (2*R*,3*R*)-tartaric acid [(VIII), orthorhombic $P2_12_12_1$, $Z' = 1$] has 3:4 stoichiometry and contains four different types of ion, $[\{HN(CH_2CH_2)_3NH\}^{2+}]_2\cdot[N(CH_2CH_2)_3NH]^{+}\cdot 3(C_4H_5O_6)^{-}\cdot C_4H_4O_6^{2-}$: the hard hydrogen bonds generate a three-dimensional framework.

1. Introduction

In hydrogen-bonded adducts of simple bis-phenols or dicarboxylic acids with tertiary diamines, the primary mode of supramolecular aggregation is chain formation by hard (Braga *et al.*, 1995) O—H···N and/or N—H···O hydrogen bonds (Coupar *et al.*, 1997; Ferguson *et al.*, 1997, 1998; Glidewell *et al.*, 1999; Lavender *et al.*, 1999). The mutual disposition of the hydrogen-bonded chains is often determined by soft (Braga *et al.*, 1995) hydrogen bonds, usually of C—H···O type or by aromatic $\pi\cdots\pi$ stacking interactions.

Where both components in such a system are achiral, the adducts generally crystallize in centrosymmetric space groups, as the occurrence of inversion centres, especially unoccupied inversion centres, seems to be particularly favourable in molecular crystals (Brock & Dunitz, 1994). Similar considerations apply if one component of such a system is a racemic mixture of the two enantiomers of a chiral building block (Burchell *et al.*, 2000, 2001). However, if one or other component is a single enantiomer of a chiral acid or amine, then this places major constraints on the range of accessible

Table 1
Experimental details.

	(I)	(II)	(III)	(IV)
Crystal data				
Chemical formula	$C_{16}H_{16}N_2O_6$	$C_{12}H_{11}N_2\cdot C_{12}H_{10}N_2\cdot C_4H_6O_6\cdot C_4H_5O_6$	$C_{10}H_9N_2\cdot C_4H_5O_6$	$C_{14}H_{14}N_2O_6$
Chemical formula weight	332.31	664.62	306.27	306.27
Cell setting, space group	Triclinic, $P\overline{1}$	Triclinic, $P1$	Triclinic, $P\overline{1}$	Monoclinic, $P2_1$
a, b, c (Å)	8.8780 (11), 9.6130 (13), 10.1020 (13)	8.6195 (3), 9.5654 (4), 9.8727 (4)	4.7847 (2), 10.2505 (5), 13.8412 (8)	10.4430 (13), 4.4665 (6), 14.110 (2)
α, β, γ (°)	73.665 (7), 66.433 (8), 79.141 (6)	103.1622 (18), 109.9123 (18), 90.262 (3)	99.434 (2), 91.252 (2), 96.163 (2)	90, 92.954 (5), 90
V (Å^3)	755.51 (17)	742.22 (5)	665.26 (6)	657.27 (15)
Z	2	1	2	2
D_x (Mg m^{-3})	1.461	1.487	1.529	1.548
Radiation type	Mo $K\alpha$	Mo $K\alpha$	Mo $K\alpha$	Mo $K\alpha$
No. of reflections for cell parameters	2118	3134	2831	1394
θ range (°)	2.98–25.05	2.74–27.46	2.99–27.93	3.41–26.42
μ (mm^{-1})	0.113	0.115	0.121	0.123
Temperature (K)	150 (2)	150 (2)	150 (2)	150 (2)
Crystal form, colour	Needle, colourless	Needle, colourless	Plate, colourless	Block, colourless
Crystal size (mm)	0.40 × 0.14 × 0.10	0.24 × 0.14 × 0.10	0.40 × 0.20 × 0.08	0.25 × 0.22 × 0.20
Data collection				
Diffractometer	Kappa-CCD	Kappa-CCD	Kappa-CCD	Kappa-CCD
Data collection method	φ scans, and ω scans with κ offsets	φ scans, and ω scans with κ offsets	φ scans, and ω scans with κ offsets	φ scans, and ω scans with κ offsets
Absorption correction	Multi-scan	Multi-scan	Multi-scan	Multi-scan
T_{min}	0.9561	0.9728	0.9530	0.9699
T_{max}	0.9888	0.9886	0.9904	0.9758
No. of measured, independent and observed reflections	5383, 2621, 1709	8988, 3390, 1944	8786, 3049, 1936	11 845, 1394, 1022
Criterion for observed reflections	$I > 2\sigma(I)$	$I > 2\sigma(I)$	$I > 2\sigma(I)$	$I > 2\sigma(I)$
R_{int}	0.059	0.061	0.066	0.033
θ_{max} (°)	25.05	27.46	27.93	26.42
Range of h, k, l	$0 \rightarrow h \rightarrow 10$ $-10 \rightarrow k \rightarrow 11$ $-10 \rightarrow l \rightarrow 12$	$0 \rightarrow h \rightarrow 11$ $-12 \rightarrow k \rightarrow 12$ $-12 \rightarrow l \rightarrow 11$	$0 \rightarrow h \rightarrow 6$ $-13 \rightarrow k \rightarrow 13$ $-17 \rightarrow l \rightarrow 17$	$0 \rightarrow h \rightarrow 12$ $0 \rightarrow k \rightarrow 5$ $-16 \rightarrow l \rightarrow 16$
Refinement				
Refinement on	F^2	F^2	F^2	F^2
$R[F^2>2\sigma(F^2)]$, $wR(F^2)$, S	0.0523, 0.1442, 1.022	0.0491, 0.1382, 0.972	0.0475, 0.1338, 0.983	0.0479, 0.1236, 1.031
No. of reflections and parameters used in refinement	2621, 247	3390, 442	3049, 205	1394, 204
H-atom treatment	H-atom parameters constrained	H-atom parameters constrained	H-atom parameters constrained	H-atom parameters constrained
Weighting scheme	$w = 1/[\sigma^2(F_o^2) + (0.0568P)^2]$, where $P = (F_o^2 + 2F_c^2)/3$	$w = 1/[\sigma^2(F_o^2) + (0.0574P)^2]$, where $P = (F_o^2 + 2F_c^2)/3$	$w = 1/[\sigma^2(F_o^2) + (0.0653P)^2]$, where $P = (F_o^2 + 2F_c^2)/3$	$w = 1/[\sigma^2(F_o^2) + (0.0578P)^2]$, where $P = (F_o^2 + 2F_c^2)/3$
$(\Delta/\sigma)_{max}$	0.000	0.001	0.000	0.000
$\Delta\rho_{max}$, $\Delta\rho_{min}$ (e Å^{-3})	0.21, −0.229	0.298, −0.251	0.265, −0.232	0.232, −0.237
Extinction method	*SHELXL*	*SHELXL*	*SHELXL*	*SHELXL*
Extinction coefficient	0.024 (7)	0.014 (3)	0.019 (6)	0.030 (8)

	(V)	(VI)	(VII)	(VIII)
Crystal data				
Chemical formula	$C_4H_{12}N_2\cdot C_4H_4O_6$	$C_4H_{12}N_2\cdot 2C_4H_5O_6$	$C_6H_{13}N_2\cdot 2C_4H_{5.5}O_6$	$2C_6H_{14}N_2\cdot C_6H_{13}N_2\cdot 3C_4H_5O_6\cdot C_4H_4O_6$
Chemical formula weight	236.23	386.32	412.35	936.88
Cell setting, space group	Monoclinic, $P2_1$	Monoclinic, $P2_1/n$	Monoclinic, $P2_1/n$	Orthorhombic, $P2_12_12_1$
a, b, c (Å)	6.4043 (3), 9.0860 (5), 9.3734 (4)	6.5439 (3), 15.7915 (8), 7.5357 (4)	7.3240 (1), 15.9935 (3), 7.5149 (1)	8.8886 (1), 10.0973 (4), 45.2601 (7)
β (°)	109.006 (3)	94.484 (2)	94.4050 (11)	90
V (Å^3)	515.70 (4)	776.34 (7)	877.67 (2)	4062.13 (18)
Z	2	2	2	4
D_x (Mg m^{-3})	1.521	1.653	1.560	1.532
Radiation type	Mo $K\alpha$	Mo $K\alpha$	Mo $K\alpha$	Mo $K\alpha$
No. of reflections for cell parameters	1118	1794	2029	3754
θ range (°)	3.21–27.49	2.58–27.47	3.0–27.44	2.66–25.02

Table 1 (continued)

	(V)	(VI)	(VII)	(VIII)
μ (mm^{-1})	0.130	0.150	0.138	0.131
Temperature (K)	150 (2)	150 (2)	150 (2)	150 (2)
Crystal form, colour	Needle, colourless	Plate, colourless	Block, colourless	Block, colourless
Crystal size (mm)	0.28 × 0.10 × 0.08	0.24 × 0.22 × 0.08	0.38 × 0.35 × 0.32	0.34 × 0.30 × 0.26
Data collection				
Diffractometer	Kappa-CCD	Kappa-CCD	Kappa-CCD	Kappa-CCD
Data collection method	φ scans, and ω scans with κ offsets	φ scans, and ω scans with κ offsets	φ scans, and ω scans with κ offsets	φ scans, and ω scans with κ offsets
Absorption correction	Multi-scan	Multi-scan	Multi-scan	Multi-scan
T_{min}	0.9644	0.9650	0.9495	0.9569
T_{max}	0.9896	0.9881	0.9572	0.9668
No. of measured, independent and observed reflections	3749, 1241, 1061	6672, 1776, 1252	8773, 1991, 1756	15 464, 4039, 2872
Criterion for observed reflections	$I > 2\sigma(I)$	$I > 2\sigma(I)$	$I > 2\sigma(I)$	$I > 2\sigma(I)$
R_{int}	0.047	0.056	0.028	0.072
θ_{max} (°)	27.49	27.47	27.44	25.02
Range of h, k, l	$0 \rightarrow h \rightarrow 8$ $0 \rightarrow k \rightarrow 11$ $-12 \rightarrow l \rightarrow 11$	$0 \rightarrow h \rightarrow 8$ $0 \rightarrow k \rightarrow 20$ $-9 \rightarrow l \rightarrow 9$	$0 \rightarrow h \rightarrow 9$ $0 \rightarrow k \rightarrow 20$ $-9 \rightarrow l \rightarrow 9$	$0 \rightarrow h \rightarrow 10$ $0 \rightarrow k \rightarrow 12$ $0 \rightarrow l \rightarrow 53$
Refinement				
Refinement on	F^2	F^2	F^2	F^2
$R[F^2>2\sigma(F^2)]$, $wR(F^2)$, S	0.0369, 0.0883, 1.034	0.0429, 0.1444, 1.104	0.036, 0.094, 1.057	0.0412, 0.0929, 1.015
No. of reflections and parameters used in refinement	1241, 148	1776, 121	1991, 162	4039, 588
H-atom treatment	H-atom parameters constrained	H-atom parameters constrained	H-atom parameters constrained	H-atom parameters constrained
Weighting scheme	$w = 1/[\sigma^2(F_o^2) + (0.0293P)^2]$, where $P = (F_o^2 + 2F_c^2)/3$	$w = 1/[\sigma^2(F_o^2) + (0.0756P)^2]$, where $P = (F_o^2 + 2F_c^2)/3$	$w = 1/[\sigma^2(F_o^2) + (0.0365P)^2 + 0.3876P]$, where $P = (F_o^2 + 2F_c^2)/3$	$w = 1/[\sigma^2(F_o^2) + (0.0417P)^2 + 0.4863P]$, where $P = (F_o^2 + 2F_c^2)/3$
$(\Delta/\sigma)_{max}$	0.000	0.000	0.001	0.001
$\Delta\rho_{max}$, $\Delta\rho_{min}$ (e Å^{-3})	0.193, −0.18	0.288, −0.282	0.297, −0.299	0.244, −0.23
Extinction method	*SHELXL*	None	None	None
Extinction coefficient	0.057 (18)	0	0	0

space groups. Overall there is a very high likelihood that the use of a single enantiomeric form of one component will lead to a different space group, and hence a different supramolecular arrangement, from that found with a racemic component.

Tartaric acid (2,3-dihydroxy-1,4-butanedioic acid, $C_4H_6O_6$) is one of the simplest chiral dicarboxylic acids, and it is readily available in the form of two single enantiomers (2*R*,3*R*) and (2*S*,3*S*) and as a racemic mixture of the two: a centrosymmetric *meso* form (2*R*,3*S*) also exists. While there are a considerable number of structure reports on salts of tartaric acid with organic bases, and with cationic metal-coordination complexes, in the vast majority of these studies the tartrate ion was present as a stereochemical indicator, since the objective of the study was determination of the absolute configuration of the cationic component. There have been few, if any, systematic studies designed to explore the structural effects of using chiral *versus* racemic tartaric acids as building blocks for supramolecular chemistry, although, Aakeröy *et al.* (1992) reported the synthesis of a long series of salts of (2*R*,3*R*)-tartaric acid in an exploration of materials for second-harmonic generation. Overall, it is striking how few structural studies have involved racemic tartaric acid, by comparison with the large number involving a single enantiomer.

As part of an investigation of chiral *versus* racemic building blocks, we report here the synthesis and structures of the salt-type adducts formed between tartaric acid and *trans*-1,2-bis(4′-pyridyl)ethene ($NC_5H_4CHCHC_5H_4N$), adducts (I) and (II); 4,4′-bipyridyl ($NC_5H_4C_5H_4N$), adducts (III) and (IV); piperazine [$HN(CH_2CH_2)_2NH$], adducts (V) and (VI); 1,4-diazabicyclo[2.2.2]octane [DABCO, $N(CH_2CH_2)_3N$], adducts (VII) and (VIII): of these products (I), (III), (VI) and (VII) involve the racemic acid, the remainder the (2*R*,3*R*) enantiomer. Hence, there are four pairs of compounds and each pair involves a common diamine with either racemic tartaric acid or (2*R*,3*R*)-tartaric acid. In the present study, the rationale informing the use of bis-tertiary or bis-heteroaromatic amines is the attempt to constrain the acid–base interactions to chain-formation only, in order to render the resulting supramolecular structures as simple as possible, the better to assess the effect of using chiral *versus* racemic building blocks, in such cases as corresponding pairs of salts can be prepared in suitable crystalline form. In the context of the space groups which are available for salts of chiral and racemic tartaric acids, it may be noted here that pure (2*R*,3*R*)-tartaric acid crystallizes in space group $P2_1$ (Okaya *et al.*, 1966), while the pure *meso* acid crystallizes in space group $P\bar{1}$ (Bootsma & Schoone, 1967).

Table 2
Hydrogen-bond parameters.

D—H···A	H···A	D···A	D—H···A
(I)			
N11—H11···O1	1.75	2.628 (2)	175
O3—H3···N21^{i}	1.81	2.645 (3)	172
O5—H5···O1	2.25	2.677 (2)	112
O5—H5···O1^{ii}	2.04	2.748 (3)	142
O6—H6···O2^{iii}	1.92	2.731 (3)	162
C27—H27···O6^{iv}	2.43	3.359 (3)	165
(II)			
N31—H31···O11	1.73	2.607 (5)	172
N41—H41···O23^{v}	1.73	2.602 (4)	172
O11—H11···N31	1.80	2.607 (5)	162
O13—H13···N61^{vi}	1.75	2.583 (5)	170
O21—H21···N51	1.279†	2.551 (5)	173
O15—H15···O26^{iv}	1.97	2.806 (4)	176
O16—H16···O25	1.95	2.781 (4)	169
O25—H25···O22	2.09	2.597 (4)	119
O26—H26···O23	2.08	2.595 (4)	119
C42—H42···O11^{vii}	2.42	3.241 (5)	145
C45—H45···O15^{viii}	2.45	3.243 (5)	141
C53—H53···O16^{viii}	2.43	3.320 (6)	156
C62—H62···O21^{vii}	2.37	3.202 (5)	145
(III)			
N11—H11···O1	1.66	2.544 (2)	177
O1—H1···N11	1.71	2.544 (2)	175
O3—H3···N21^{ix}	1.78	2.614 (2)	174
O5—H5···O2	2.22	2.693 (2)	116
O5—H5···O2^{x}	2.07	2.823 (2)	149
O6—H6···O5^{xi}	1.90	2.740 (2)	173
C16—H16···O1^{xii}	2.36	3.279 (3)	164
C23—H23···O4^{xii}	2.50	3.448 (3)	175
(IV)			
N11—H11···O1	1.60	2.479 (4)	178
O1—H1···N11	1.64	2.479 (4)	176
O3—H3···N21^{xiii}	1.72	2.550 (4)	171
O5—H5···O2	2.08	2.586 (4)	118
O5—H5···O2^{xiv}	2.21	2.929 (4)	144
O6—H6···O5^{xv}	1.78	2.619 (4)	176
C15—H15···O4^{xvi}	2.43	3.375 (5)	170
C23—H23···O4^{xvi}	2.40	3.262 (5)	150
(V)			
N11—H11*A*···O4	1.84	2.686 (2)	152
N11—H11*B*···O1^{xvii}	1.87	2.759 (3)	161
N14—H14*A*···O2^{xviii}	1.86	2.773 (3)	170
N14—H14*B*···O3^{xi}	1.93	2.775 (3)	153
O5—H5···O1	2.13	2.628 (3)	118
O5—H5···O2^{xix}	2.25	2.962 (2)	143
O6—H6···O4	2.10	2.613 (2)	119
O6—H6···O2^{xi}	2.35	2.965 (2)	130
(VI)			
N1—H1*A*···O5	1.91	2.772 (2)	155
N1—H1*B*···O3^{xx}	1.88	2.801 (2)	174
O1—H1···O3^{xxi}	1.72	2.558 (2)	173
O5—H5···O2^{xxii}	2.02	2.727 (2)	142
O6—H6···O4^{xxiii}	1.90	2.696 (2)	158
(VII)			
N1—H1*A*···O3	1.90	2.701 (5)	142
N1—H1*A*···O6	2.25	2.977 (4)	135
N2—H2*A*···O3^{xxiv}	2.10	2.813 (5)	132
N2—H2*A*···O6^{xxiv}	1.93	2.711 (5)	141
O1—H1···O3^{xvii}	1.69	2.527 (2)	173
O5—H5···O2	2.37	2.684 (2)	103
O5—H5···O2^{xxv}	2.11	2.866 (2)	149
O6—H6···O4^{xxvi}	1.88	2.702 (2)	166
C11—H11*A*···O5^{xx}	2.46	2.709 (3)	94
C11—H11*B*···O5^{xx}	2.55	2.709 (3)	88
C21—H21*A*···O5^{xx}	2.81	2.775 (3)	78
C21—H21*B*···O5^{xx}	2.42	2.775 (3)	100
(VIII)			
N51—H51···O13	2.08	2.858 (4)	141
N51—H51···O16	2.21	2.911 (4)	132
N61—H61···O24	1.71	2.640 (4)	174
N62—H62···O34	1.71	2.625 (4)	166
N71—H71···O31	1.64	2.551 (4)	166
N72—H72···O43	2.14	2.895 (4)	137
N72—H72···O46	1.98	2.759 (4)	140
O21—H21···N52	1.82	2.656 (4)	178
O14—H14···O12^{xxvii}	1.66	2.489 (3)	171
O15—H15···O12	2.34	2.691 (3)	106
O15—H15···O42^{xxviii}	2.09	2.837 (4)	148
O16—H16···O41^{xxix}	2.03	2.761 (4)	145
O25—H25···O32^{xxx}	1.98	2.803 (4)	168
O26—H26···O24	2.20	2.643 (4)	113
O26—H26···O34^{iv}	2.12	2.791 (3)	136
O35—H35···O31	2.14	2.619 (4)	116
O35—H35···O23^{xxx}	2.15	2.874 (4)	144
O36—H36···O24^{xv}	2.07	2.768 (3)	141
O36—H36···O34	2.18	2.643 (4)	114
O44—H44···O42^{xxxi}	1.69	2.523 (3)	170
O45—H45···O42	2.14	2.635 (4)	118
O45—H45···O12^{xxxii}	2.29	2.982 (4)	141
O46—H46···O11^{xxxiii}	1.79	2.603 (4)	162

Symmetry codes: (i) $x, 2+y, -1+z$; (ii) $1-x, 2-y, 1-z$; (iii) $-x, 2-y, 1-z$; (iv) $x, -1+y, z$; (v) $-1+x, 1+y, 1+z$; (vi) $1+x, -2+y, -1+z$; (vii) $x, 1+y, 1+z$; (viii) $-1+x, 1+y, z$; (ix) $2+x, y, -1+z$; (x) $2-x, 1-y, 1-z$; (xi) $-1+x, y, z$; (xii) $1-x, -y, 1-z$; (xiii) $x, -2+y, 1+z$; (xiv) $-x, -\frac{1}{2}+y, 1-z$; (xv) $x, 1+y, z$; (xvi) $1-x, \frac{3}{2}+y, 1-z$; (xvii) $x, y, 1+z$; (xviii) $-1+x, y, 1+z$; (xix) $2-x, -\frac{1}{2}+y, -z$; (xx) $1+x, y, z$; (xxi) $x, y, -1+z$; (xxii) $-x, 1-y, -z$; (xxiii) $-\frac{1}{2}+x, \frac{3}{2}-y, -\frac{1}{2}+z$; (xxiv) $1-x, 1-y, 1-z$; (xxv) $-x, 1-y, 2-z$; (xxvi) $\frac{1}{2}+x, \frac{3}{2}-y, \frac{1}{2}+z$; (xxvii) $1-x, -\frac{1}{2}+y, \frac{1}{2}-z$; (xxviii) $\frac{1}{2}-x, 1-y, -\frac{1}{2}+z$; (xxix) $\frac{3}{2}-x, 1-y, -\frac{1}{2}+z$; (xxx) $\frac{1}{2}+x, \frac{3}{2}-y, 1-z$; (xxxi) $1-x, \frac{1}{2}+y, \frac{3}{2}-z$; (xxxii) $\frac{1}{2}-x, 1-y, \frac{1}{2}+z$; (xxxiii) $\frac{3}{2}-x, 1-y, \frac{1}{2}+z$. † O21—H21 1.277 Å

2. Experimental

2.1. Synthesis

Equimolar quantities of the appropriate tartaric acid [(2*R*,3*R*) or racemic] and the appropriate amine were separately dissolved in methanol: the solutions were mixed and set aside to crystallize, giving analytically pure samples of (I)–(VIII). Analyses: (I), found C 58.2, H 4.9, N 8.5%; $C_{16}H_{16}N_2O_6$ requires C 57.8, H 4.9, N 8.4%; (II), found C 57.9, H 4.9, N 8.5%; $C_{16}H_{16}N_2O_6$ requires C 57.8, H 4.9, N 8.4%; (III), found C 54.9, H 4.5, N 9.2%; $C_{14}H_{14}N_2O_6$ requires C 54.9, H 4.6, N 9.2%; (IV), found C 55.2, H 4.4, N 9.1%; $C_{14}H_{14}N_2O_6$ requires C 54.9, H 4.6, N 9.2%; (V), found C 37.7, H 5.8, N 7.3; $C_{12}H_{22}N_2O_6$ requires C 37.3, H 5.7, N 7.3%; (VI), found C 39.7, H 6.6, N 11.3%; $C_8H_{16}N_2O_6$ requires C 40.7, H 6.8, N 11.9%; (VII), found C 40.7, H 5.8, N 6.8%; $C_{14}H_{24}N_2O_6$ requires C 40.8, H 5.9, N 6.8%; (VIII), found C 48.5, H 7.0, N 9.6%; $C_{34}H_{60}N_6O_{24}$ requires C 48.6, H 7.2, N 10.0%. Crystals suitable for single-crystal X-ray diffraction were selected directly from the analytical samples.

2.2. Data collection, structure solution and refinement

Diffraction data for (I)–(VIII) were collected at 150 (2) K using a Nonius Kappa-CCD diffractometer with graphite-monochromated Mo K_α radiation (λ = 0.71073 Å). Other

details of cell data, data collection and refinement are summarized in Table 1, together with details of the software employed (Ferguson, 1999; Nonius, 1997; Otwinowski & Minor, 1997; Sheldrick, 1997*a*,*b*; Spek, 2001). Compounds (I)–(III) are all triclinic; for (I) and (III) the space group $P\bar{1}$ was assumed and confirmed by the structure analysis, while for (II) the space group $P1$ was chosen and confirmed by the analysis. For (IV) and (V), the systematic absences permitted $P2_1$ and $P2_1/m$ as possible space groups and, in both cases, $P2_1$ was chosen and confirmed by the analysis. For (VI), (VII) and (VIII), space groups $P2_1/n$, $P2_1/n$ and $P2_12_12_1$, respectively, were uniquely assigned from the systematic absences. The structures were solved by direct methods and refined with all data on F^2. A weighting scheme based upon $P = [F_o^2 + 2F_c^2]/3$ was employed in order to reduce statistical bias (Wilson, 1976). The asymmetric unit of (VII) contains one tartrate anion [chosen to have the (2*R*,3*R*) configuration] and one half of a DABCO molecule which lies about an inversion centre and is disordered so that the atoms have 0.5 occupancy; to ensure sensible geometry the N—C and C—C distances were restrained to have common values by means of *DFIX* commands coupled with free-variable refinement. Refined values were 1.492 (4) (C—N) and 1.523 (4) (C—C). In (I) the anion is disordered over two sets of sites with refined site-occupation factors 0.0.915 (2) and 0.085 (2) and it was not possible to locate H atoms bonded to O in the minor form. In (II) the H atom H21 was found to lie equidistant from O21 and N51. All other H atoms were located from difference maps and included in the refinements as riding atoms with O—H 0.84, N—H 0.88–0.93 and C—H 0.95–1.00 Å. The refined values of the Flack parameter (Flack, 1983) for (II), (IV), (V) and (VIII) [−0.5 (16), 0 (2), −0.6 (14) and 2.8 (12), respectively] were all inconclusive (Flack & Bernardinelli, 2000) and hence the Friedel equivalents were merged before the final refinements for these compounds. The diagrams were prepared with the aid of *PLATON* (Spek, 2001). Details of the hydrogen-bond dimensions are given in Table 2.[1]

3. Results and discussion

3.1. Compositions and constitutions

For all syntheses, equimolar quantities of the diamine and the tartaric acid components were employed, in the expectation that 1:1 stoichiometries might result, containing equal numbers of strongly acidic carboxyl groups and amine acceptors. In the event, 1:1 stoichiometries were consistently observed only with 4,4′-bipyridyl and 1,2-bis(4-pyridyl)ethene, (I)–(IV): for each of the saturated amines piperazine and 1,4-diazabicyclo[2.2.2]octane (DABCO), the stoichiometry of the product obtained using (2*R*,3*R*)-tartaric acid differed from that obtained using the racemic acid. The chiral tartaric acid forms a 1:1 product, (V) with piperazine, consistent with those formed by the bis-pyridyl species, but with the racemic acid, both piperazine and DABCO form 1:2 products; (VI) and (VII), having two acid units per diamine: by contrast to these rather simple compositions, (2*R*,3*R*)-tartaric acid forms an unexpected 3:4 product, (VIII), with DABCO. It may be noted that none of the foregoing products contains any solvent-derived components.

In a 1: 1 adduct formed by a diacid AH_2 with a diamine B, it might reasonably be expected that double transfer of H from O to N would occur, giving a salt of the type $[BH_2]^{2+}\cdot[A]^{2-}$. However, in (I) only a single H transfer has occurred to yield a product of the type $[BH]^{+}\cdot[AH]^{-}$, while in (II) two partial transfers of H have occurred, manifested in one case by an almost centred O···H···N array and in the other by an H disordered over two sites having unequal occupancy, thus giving rise to the constitution $[BH_{0.5}]^{0.5+}\cdot[BH_{1.3}]^{1.3+}\cdot[AH_{0.5}]^{1.5-}\cdot[AH_{1.7}]^{0.3-}$. Again, in (III) and (IV) the H transfers from O to N are only partial, giving rise to constitutions of the types $[BH_{0.6}]^{0.6+}\cdot[AH_{1.4}]^{0.6-}$ and $[BH_{0.5}]^{0.5+}\cdot[AH_{1.5}]^{0.5-}$, respectively.

Both the unsolvated 1:2 adducts (VI) and (VII), formed by piperazine and DABCO, are characterized by simple ionic constitutions $[BH_2]^{2+}\cdot[(AH)^{-}]_2$, and similarly the 1:1 product (V) formed by piperazine has the simple constitution $[BH_2]^{2+}\cdot[A]^{2-}$: it may be noted here that compound (V) is the

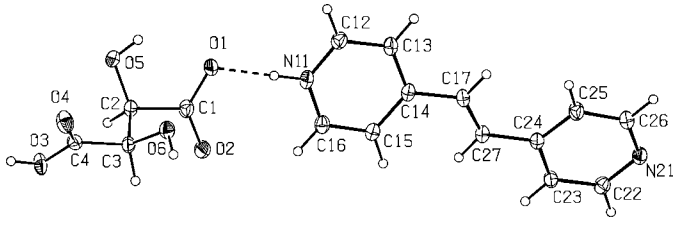

Figure 1
The molecular components of (I) showing the atom-labelling scheme. For the sake of clarity the minor conformer of the anion (atoms C31–C34, O31–O36) is omitted. Displacement ellipsoids are drawn at the 30% probability level.

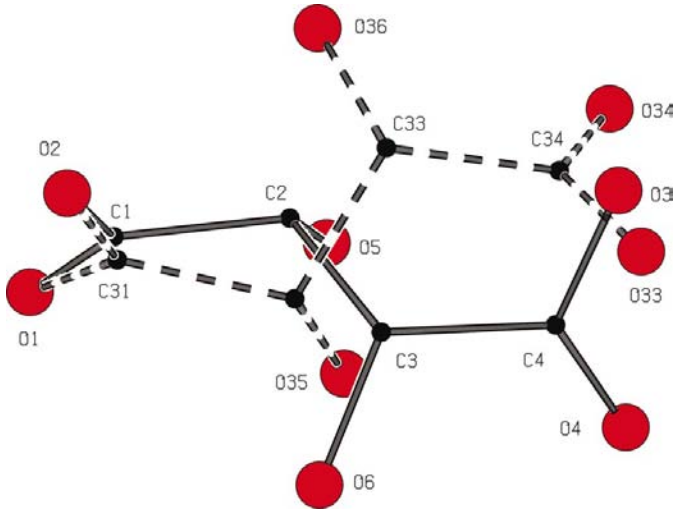

Figure 2
The two orientations of the anion in (I), showing the common sites for O1/O31 and O2/O32. For the sake of clarity, H atoms are omitted and the atoms are depicted as spheres of arbitrary radius, C < O.

[1] Supplementary data for this paper are available from the IUCr electronic archives (Reference: NA0130). Services for accessing these data are described at the back of the journal.

only example so far encountered in this series which has 1:1 stoichiometry with the simple $[BH_2]^{2+}\cdot[A]^{2-}$ constitution. Both the 3:4 composition of (VIII) and its constitution $[(BH_2)^{2+}]_2\cdot[(BH)^{+}]\cdot[(AH)^{-}]_3\cdot[A]^{2-}$ are wholly unexpected and entirely unpredictable.

3.2. Supramolecular structures

3.2.1. Salts of 1,2-bis(4′-pyridyl)ethene: hard hydrogen bonds generate sheets. Racemic tartaric acid forms a 1: 1 salt with 1,2-bis(4′-pyridyl)ethene in which a single H transfer has occurred to give the product (I) $[(C_{12}H_{10}N_2)H]^{+}\cdot[C_4H_5O_6]^{-}$ (Fig. 1), which crystallizes in the space group $P\bar{1}$ so that equal numbers of (2*R*, 3*R*) and (2*S*, 3*S*) anions are present. The anion is disordered over two sets of sites, whose refined site occupation factors are 0.915 (2) and 0.085 (2), such that the O atom sites of one carboxyl group are common to both orientations (Fig. 2). Owing to the very low occupancy of the minor form, only the major form will be considered in the discussion of the supramolecular organization.

Apart from an intra-anion O—H···O hydrogen bond (Table 2) which serves partially to lock and control the conformation of the anion, the supramolecular structure is generated by four hard hydrogen bonds and one soft C—H···O hydrogen bond. Within the asymmetric unit (Fig. 1) there is a short and nearly linear N—H···O hydrogen bond, whose strength is a consequence of both donor and acceptor being charged, thus N^{+}—H···O^{-} (Aakeröy & Seddon, 1993; Gilli *et al.*, 1994). Two O—H···O hydrogen bonds and one O—H···N hydrogen bond generate sheets and these sheets are linked by the C—H···O hydrogen bonds. It is convenient to consider the formation of the two-dimensional structure in terms of the one-dimensional substructure generated by the anions alone and the linking of the anion chains by the cation.

In the reference anion at (*x*, *y*, *z*), which is of (2*R*, 3*R*) type (Fig. 1), hydroxylic O5 and O6 act as hydrogen-bond donors, respectively, to O1 at $(1-x, 2-y, 1-z)$ and to O2 at $(-x, 2-y, 1-z)$. Propagation of these interactions produces a chain of fused rings running parallel to the [100] direction in which there are $R_2^2(12)$ rings centred at (*n*, 1, 0.5; *n* = zero or integer) alternating with $R_2^2(10)$ rings centred at $(n+\frac{1}{2}, 1, \frac{1}{2}$; *n* = zero or integer) and in which (2*R*, 3*R*) and (2*S*, 3*S*) anions alternate (Fig. 3).

Chains of this type are linked by the cations. N11 at (*x*, *y*, *z*) acts as a hydrogen-bond donor to O1, also at (*x*, *y*, *z*), while N21 in the same cation at (*x*, *y*, *z*) acts as an acceptor from O3 in the anion at $(x, -2+y, 1+z)$. Similarly O3 in the anion at (*x*, *y*, *z*) acts as a donor to N21 in the cation at $(x, 2+y, -1+z)$ and hence a $C_2^2(18)$ chain is generated by translation, running parallel to the $[02\bar{1}]$ direction. The combination of the [100] chains of anions and the $[02\bar{1}]$ chains of alternating cations and anions generates a (012) sheet (Fig. 3) in which the antiparallel cations are separated by large centrosymmetric rings, alternately of $R_6^6(40)$ and $R_6^4(38)$ types, centred for example at (*n*, 0, 1) and $(n+\frac{1}{2}, 0, 1)$, respectively (*n* = zero or integer).

The (012) sheets are linked into a single three-dimensional framework by a single C—H···O hydrogen bond. Atom C27 in the cation at (*x*, *y*, *z*), part of the ethene spacer unit between the heteroaromatic rings, acts as hydrogen-bond donor to O6 at $(x, -1+y, z)$, which lies in the adjacent (012) sheet in the $[0\bar{1}0]$ direction. Similarly, atom C27 at $(1-x, -y, 2-z)$, which is also a component of the reference (012) sheet, acts as a hydrogen-bond donor to O6 at $(1-x, 1-y, 2-z)$, a component of the adjacent (012) sheet in the [010] direction. In this manner, each (012) sheet is linked to its two immediate

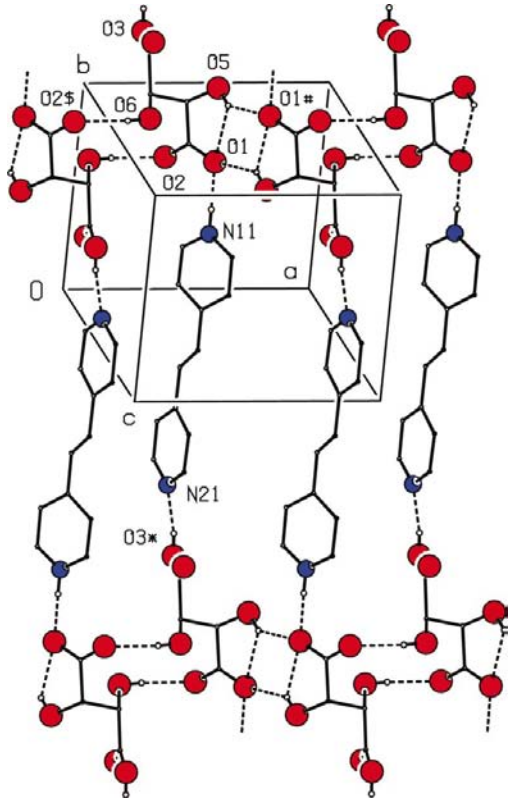

Figure 3
Part of the crystal structure of (I) showing the formation of a (012) sheet by hard hydrogen bonds. For the sake of clarity, H atoms bonded to C are omitted. The atoms marked with an asterisk (*), hash (#) or dollar sign ($) are at the symmetry positions $(x, -2+y, 1+z)$, $(1-x, 2, -y, 1-z)$ and $(-x, 2-y, 1-z)$, respectively.

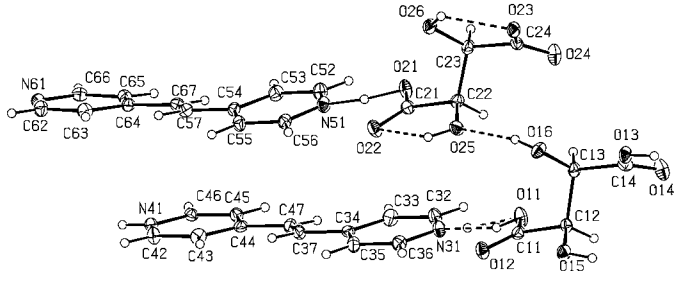

Figure 4
The molecular components of (II) showing the atom-labelling scheme. Displacement ellipsoids are drawn at the 30% probability level. The H atom between O11 and N31 is disordered over two sites with occupancies 0.69 (7) and 0.31 (7) adjacent to O and N, respectively.

neighbours, thus generating a continuous three-dimensional framework.

The 1:1 adduct formed between (2*R*,3*R*)-tartaric acid and 1,2-bis(4′-pyridyl)ethene (II) crystallizes in the triclinic space group *P*1. Several data sets were collected for this compound, using different crystals, as it was possible to index the data using a value of *b* half that given in Table 1: using such a data set, it was possible to solve and refine the structure apparently satisfactorily. When the dataset collected using the larger cell was carefully scrutinized, it was found that the *hkl* reflections with *k* odd were all weak to non-observed: nonetheless, some of these reflections were undoubtedly present. Using the larger cell, the structure was solved and refined in space group *P*1 with $Z' = 2$, to give an asymmetric unit (Fig. 4) in which the non-H atoms of the two tartrate units and of the two bispyridyl units were virtually superimposable. There are significant differences only in the positions of the eight H atoms bonded to N and/or O and it is these H atoms which are, in effect, solely responsible for the weak but observed *k* = odd reflections.

The H atoms attached to O25 and O26 participate in intramolecular O—H···O hydrogen bonds, but otherwise play no role. The H atom between O21 and N51 occupies a single site almost equidistant from O and N; the H between O11 and N31, on the other hand, occupies two sites with normal O—H and N—H distances, having occupancies of 0.69 (7) and 0.31 (7), respectively. The H between O16 and O25 is fully ordered and bonded to O16. Hence there are just three H atoms on O13, O15 and N41 available for the formation of hard inter-aggregate hydrogen bonds. These hydrogen bonds generate sheets and two pairs of C—H···O hydrogen bonds link the sheets into a three-dimensional framework. As with (I) it is convenient to consider in (II) firstly the one-dimensional anion structure, then the linking of the anion chains into sheets and finally the linking of the sheets.

Within the asymmetric unit (Fig. 4), atom O16 acts as a hydrogen-bond donor to O25: at the same time, O15 at (x, y, z) acts as a hydrogen-bond donor to O26 at $(x, -1 + y, z)$. These two O—H···O hydrogen bonds thus generate, by translation, a $C_2^2(10)$ chain running parallel to the [010] direction and in which the two independent anions alternate, one acting as a double donor of hydrogen bonds and the other as a double acceptor (Fig. 5). It is important to draw attention to the differences between the anion chains in (I) and (II) (Figs. 3 and 5). In (I) the chain of fused rings is propagated by inversion and alternate anions are enantiomeric, although having identical hydrogen-bonding characteristics; in (II) the anion chain is propagated by translation only and alternate anions, although having entirely different hydrogen-bonding characteristics, are of the same chirality. Likewise the linking of the anion chains into sheets and the subsequent linking of the sheets also show some subtle differences between (I) and (II).

In (II) (Fig. 4), O11 and O21 are linked to N31 and N51, respectively. At the distal ends of these bipyridine units, N61 at (x, y, z) acts as an acceptor from O13 at $(-1 + x, 2 + y, 1 + z)$, thus generating a $C_3^3(21)$ chain running parallel to the $[\bar{1}21]$ direction: N41 at (x, y, z) acts as a donor to O23 at $(-1 + x, 1 + y, 1 + z)$, thus generating a $C_4^3(22)$ chain also parallel to $[\bar{1}21]$ (Fig. 5). Each type of $[\bar{1}21]$ chain involves just one type of bispyridine, but both types of tartrate. The combination of the [010] anion chains and the two $C_3^3(21)$ chains of cations and anions generates a (101) sheet containing $R_6^6(44)$ and $R_8^8(44)$ rings. Each (101) sheet is linked to the two adjacent sheets by pairs of C—H···O hydrogen bonds. Atoms C42 and C62 in the two bispyridylethene units at (x, y, z) act as hydrogen-bond donors to O11 and O21, respectively, at

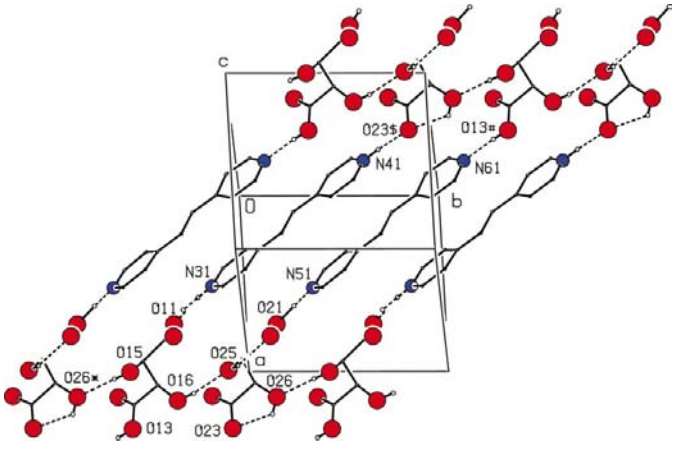

Figure 5
Part of the crystal structure of (II) showing the formation of a (101) sheet by hard hydrogen bonds. For the sake of clarity, H atoms bonded to C are omitted. The atoms marked with an asterisk (*), hash (#) or dollar sign ($) are at the symmetry positions $(x, -1 + y, z)$, $(-1 + x, 2 + y, 1 + z)$ and $(-1 + x, 1 + y, 1 + z)$, respectively.

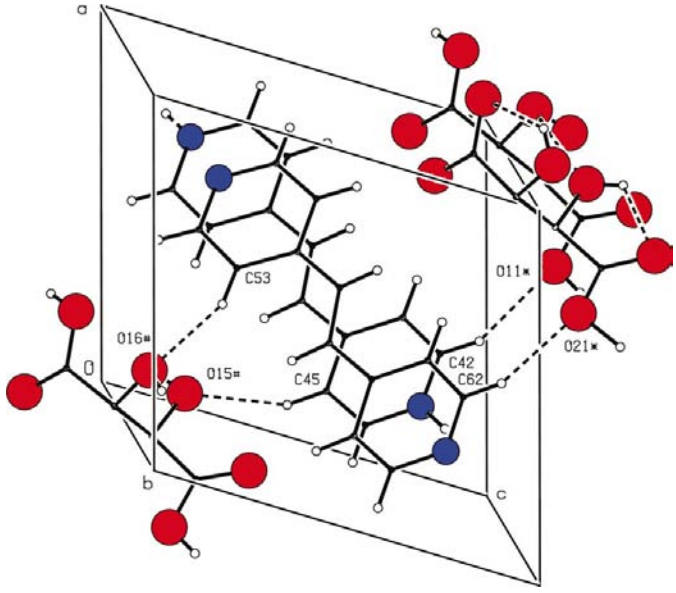

Figure 6
Part of the crystal structure of (II) showing the linking of the (101) sheets by soft hydrogen bonds. For the sake of clarity, H atoms bonded to C in the anions are omitted. The atoms marked with an asterisk (*) or hash (#) are at the symmetry positions $(x, 1 + y, 1 + z)$ and $(-1 + x, 1 + y, z)$, respectively.

$(x, 1 + y, 1 + z)$, components of the adjacent sheet in the [001] direction, while C45 and C53 at (x, y, z) act as donors to O15 and O16, respectively, at $(-1 + x, 1 + y, z)$, components of the adjacent (101) sheet in the opposite direction (Fig. 6). Hence all the sheets are linked into a continuous three-dimensional framework.

In (I) and (II), therefore, with a common broad pattern of the two supramolecular structures, comprising one-dimensional anion motifs linked by the cations into sheets, and thence by the C—H···O hydrogen bonds into frameworks, the supramolecular structures differ significantly in every detail, including not only the value of Z' but the detailed arrangement of both the hard and soft hydrogen bonds.

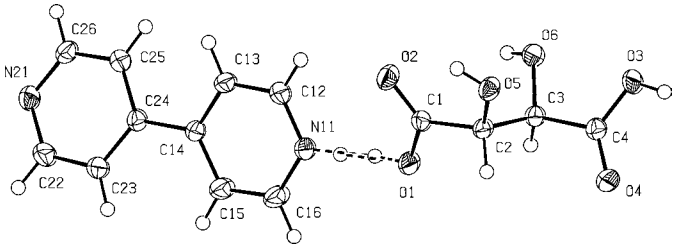

Figure 7
The molecular components of (III) showing the atom-labelling scheme. Displacement ellipsoids are drawn at the 30% probability level. The H atom between O1 and N31 is disordered over two sites with occupancies 0.40 (4) and 0.60 (4) adjacent to O and N, respectively.

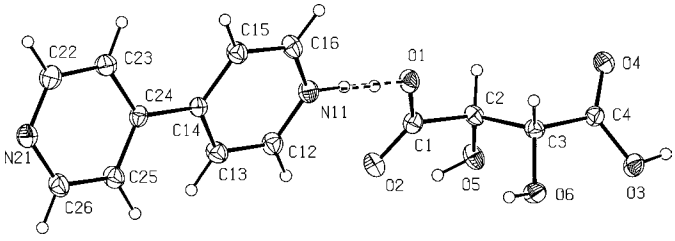

Figure 8
The molecular components of (IV) showing the atom-labelling scheme. Displacement ellipsoids are drawn at the 30% probability level. The H atom between O1 and N31 is disordered over two sites with equal occupancies.

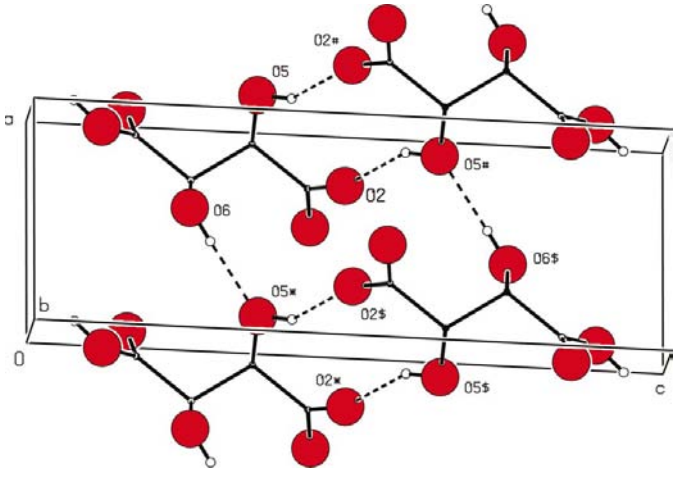

Figure 9
Part of the crystal structure of (III) showing a chain of fused $R_2^2(10)$ and $R_4^4(16)$ rings formed by the anions alone. For the sake of clarity, H atoms bonded to C are omitted. The atoms marked with an asterisk (*), hash (#) or dollar sign ($) are at the symmetry positions $(-1 + x, y, z)$, $(2 - x, 1 - y, 1 - z)$ and $(1 - x, 1 - y, 1 - z)$, respectively.

3.2.2. Salts of 4,4′-bipyridyl: hard hydrogen bonds generate bilayers. Both racemic tartaric acid and (2*R*,3*R*)-tartaric acid form 1:1 salts (III) and (IV) with 4,4′-bipyridyl, and in each salt there is only a partial transfer of H from O to N (Figs. 7 and 8), leading to disordered N—H···O/O—H···N hydrogen bonds with short N···O distances (Table 2). In the salt of the racemic acid, the H atom between O1 and N11 is disordered over two sites: the O—H and N—H distances are normal and the associated site-occupation factors are 0.40 (4) and 0.60 (4), respectively. By contrast, in the salt formed by (2*R*,3*R*)-tartaric acid, the two sites have equal occupancy. Despite the different space groups ($P\bar{1}$ and $P2_1$, respectively), at the broadest level the supramolecular structures of (III) and (IV) show a number of similarities, such that their descriptive analyses can be closely parallel: nonetheless, as for the pair of structures (I) and (II), at the detailed level there are marked differences between the structures of (III) and (IV).

In each of (III) and (IV), the anions exhibit an intramolecular O—H···O hydrogen bond: if the disordered N—H···O/O—H···N hydrogen bonds are, in each case, regarded as a single interaction, then the supramolecular structures are both generated by four hard hydrogen bonds and two soft C—H···O hydrogen bonds (Table 2). In both structures it is convenient to consider firstly chain formation by the anions,

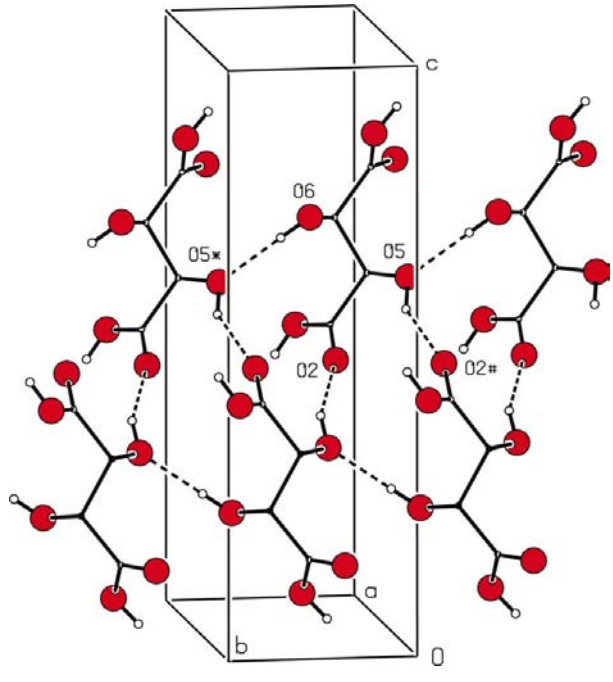

Figure 10
Part of the crystal structure of (IV) showing a [010] chain of fused $R_3^3(13)$ rings formed by the anions alone. For the sake of clarity, H atoms bonded to C are omitted. The atoms marked with an asterisk (*) or hash (#) are at the symmetry positions $(x, 1 + y, z)$ and $(-x, -\frac{1}{2} + y, 1 - z)$, respectively.

then the formation of bilayers by cations and anions, and finally the linking of the bilayers by the soft hydrogen bonds. It may be noted here that, despite the different space groups, the unit cell volumes for (III) and (IV) are very similar, as are the magnitudes of the lattice vectors, if a and b in (III) are interchanged.

In (III) the anions form a chain of fused rings, generated by inversion and translation. Hydroxyl O6 in the anion at (x, y, z) acts as a hydrogen-bond donor to hydroxyl O5 in the anion at $(-1+x, y, z)$: hydroxyl O5 at (x, y, z) acts as a donor to carboxyl O2 at $(2-x, 1-y, 1-z)$ and in this manner is produced a chain running parallel to [100]. Within the chain there are $R_2^2(10)$ rings centred at $(n, \frac{1}{2}, \frac{1}{2}; n$ = zero or integer) alternating with $R_4^4(16)$ rings centred at $(n+\frac{1}{2}, \frac{1}{2}, \frac{1}{2}; n$ = zero or integer; Fig. 9). By contrast, the anion chain in (IV) is generated by a combination of translation and the action of the twofold screw axis. Hydroxyl O6 at (x, y, z) acts as a donor to O5 at $(x, 1+y, z)$; hydroxyl O5 at (x, y, z) acts as a donor to carboxyl O2 at $(-x, -\frac{1}{2}+y, 1-z)$, while O5 at $(-x, -\frac{1}{2}+y, 1-z)$ acts as a donor to O2 at $(x, -1+y, z)$. The chain of fused rings thus produced thus runs parallel to the [010] direction and consists of just a single type of $R_3^3(13)$ ring (Fig. 10).

Within the asymmetric unit of (III) (Fig. 7), N11 and O1 are linked by the disordered H atom: in addition, the fully ordered carboxyl O3 at (x, y, z) acts as a hydrogen-bond donor to N21 at $(2+x, y, -1+z)$, thus generating a $C_2^2(16)$ chain running parallel to the $[20\bar{1}]$ direction: two such chains run through each unit cell, related to one another by the centres of inversion and thus they are strictly parallel. The chains are linked in pairs by centrosymmetric pairs of anions (Fig. 11), thus generating a $[20\bar{1}]$ chain of alternating centrosymmetric $R_2^2(10)$ and centrosymmetric $R_6^6(38)$ rings. The combination of the [100] and $[20\bar{1}]$ chains generates the bilayer parallel to (010).

The formation of the cation–anion chains in (IV) is similar to that in (III), but their linking into bilayers is different and dominated by the presence of 2_1 screw axes in (IV) rather than centres of inversion in (III). Within the asymmetric unit of (IV), N11 and O1 are linked by the disordered H (Fig. 8). Carboxyl O3 in the anion at (x, y, z) acts as a hydrogen-bond donor to N21 at $(x, -2+y, 1+z)$, thus generating a $C_2^2(16)$

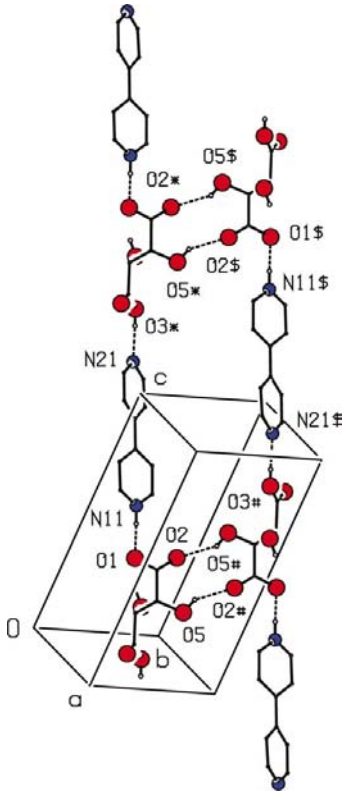

Figure 11
Part of the crystal structure of (III) showing the formation of a $[20\bar{1}]$ chain of fused $R_2^2(10)$ and $R_6^6(38)$ rings. For the sake of clarity, only the major component of the H between O1 and N11 is shown, and H atoms bonded to C are omitted. The atoms marked with an asterisk (*), hash (#) or dollar sign ($) are at the symmetry positions $(-2+x, y, 1+z)$, $(2-x, 1-y, 1-z)$ and $(-x, 1-y, 2-z)$, respectively.

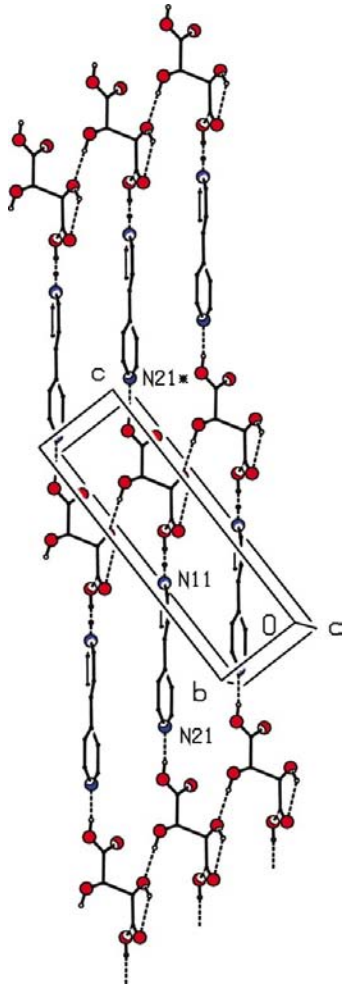

Figure 12
Part of the crystal structure of (IV) showing the formation of a (100) sheet built from $R_6^6(40)$ rings. For the sake of clarity, H atoms bonded to C are omitted. The atom marked with an asterisk (*) is at the symmetry position $(x, -2+y, 1+z)$.

chain running parallel to the [02$\bar{1}$] direction (Fig. 12). Allowing for the difference in axial orientation, this chain is entirely equivalent to the [20$\bar{1}$] chain in (III). The combination in (IV) of the [010] anion chains and the [02$\bar{1}$] cation–anion chains produces a sheet parallel to (100) generated by translation and built from a single type of $R_6^6(40)$ ring (Fig. 12). Although in (III), all of the cation–anion chains are parallel, this is not the case in (IV) as the chains here are related by the screw axes: the effect of the 2_1 axes on the set of parallel [02$\bar{1}$] chains (Fig. 12) is to generate a set of [021] chains; each (100) bilayer comprises equal numbers of [02$\bar{1}$] and [021] chains, which are pairwise linked by the [010] anion chains (Fig. 13).

As with the simple sheets in (I) and (II), so the bilayers in (III) and (IV) are linked by soft hydrogen bonds to give continuous frameworks. In (III) atoms C16 and C23 in the bipyridyl unit at (x, y, z) lie in the bilayer centred at $y = \frac{1}{2}$: these two C atoms act as hydrogen-bond donors to O1 and O4, respectively, in the anion at $(1 - x, -y, 1 - z)$, which is part of the bilayer centred at $y = -\frac{1}{2}$ (Fig. 14). Propagation of these hydrogen bonds by the centres of inversion thus links each bilayer to its two neighbours. Similarly in (IV), atoms C15 and C23 at (x, y, z) both lie in the (100) bilayer centred at $x = 0.0$: these two C atoms both act as donors to O4 in the anion at $(1 - x, \frac{3}{2} + y, 1 - z)$, which lies in the bilayer centred at $x = 1.0$, and again propagation of these hydrogen bonds links each bilayer directly to its two immediate neighbours.

3.2.3. Salts of piperazine and DABCO: hard hydrogen bonds generate three-dimensional frameworks. With racemic tartaric acid, piperazine forms a 1:2 salt $[H_2N(CH_2CH_2)_2NH_2]^{2+}\cdot[(C_4H_5O_6)^-]_2$ (VI), which crystallizes in space group $P2_1/n$ with $Z' = 0.5$. The cation lies across a centre of inversion, chosen for convenience as that at $(\frac{1}{2}, \frac{1}{2}, \frac{1}{2})$, and it thus adopts the chair conformation: all H atoms in (VI) are fully ordered. By contrast, with (2*R*,3*R*)-tartaric acid, piperazine forms a 1:1 salt $[H_2N(CH_2CH_2)_2NH_2]^{2+}\cdot[C_4H_4O_6]^{2-}$ (V) (erroneously described by Aakeröy *et al.*, 1992, as $[H_2N(CH_2CH_2)_2NH]^+\cdot[C_4H_5O_6]^-$), which crystallizes in space group $P2_1$ with $Z' = 1$. In both compounds the supramolecular aggregation can readily be analysed in terms of the substructure formed by the anions only and the subsequent influence of the cations. The principal difference between the anion substructures, reflecting the different anions present $(C_4H_5O_6)^-$ in (VI) and $(C_4H_4O_6)^{2-}$ in (V), lies in their dimensionality. In (V), where the anion has just the two hydroxyl groups available to act as hydrogen-bond donors, the O—H···O hydrogen bonds generate a two-dimensional anion substructure, while in (VI), where there is also an unionized carboxyl group, the anion framework is three-dimensional, encapsulating voids which contain the cations.

Diazabicyclo[2.2.2]octane $[N(CH_2CH_2)_3N$; DABCO] also forms a 1:2 salt with racemic tartaric acid $[HN(CH_2CH_2)_3NH]^{2+}\cdot[(C_4H_5O_6)^-]_2$ (VII), which also crystallizes in space group $P2_1/n$ with $Z' = 0.5$, with unit-cell dimensions fairly similar to those of (VI). As in (VI), the cation in (VII) lies across a centre of inversion, again selected as that at $(\frac{1}{2}, \frac{1}{2}, \frac{1}{2})$, but in this instance the cation is necessarily disordered. The supramolecular structure can again be analysed in terms of a three-dimensional anion substructure enclosing voids which contain the cations. Owing to the cation disorder in (VII) on the one hand, and on the other, the fact that in the cation of (VII) there are only two N—H bonds available for hydrogen-bond formation, whereas the cation of (VI) contains four such bonds, there are differences between these two compounds in terms of the cation–anion binding.

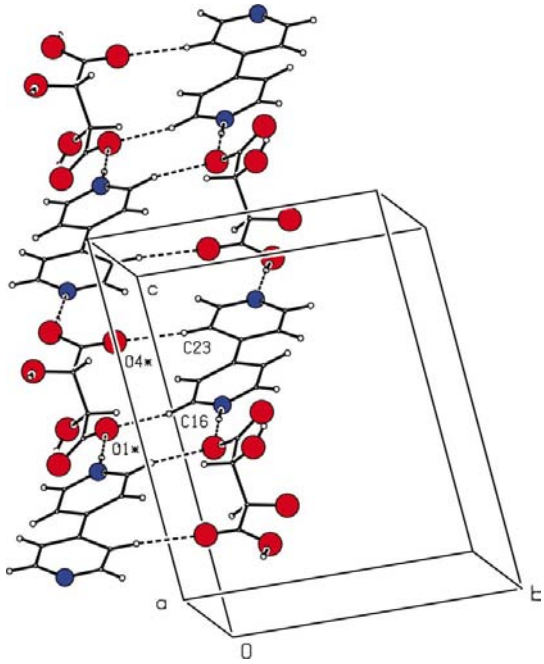

Figure 14
Part of the crystal structure of (III) showing the linking of adjacent bilayers by C—H···O hydrogen bonds. The atoms marked with an asterisk (*) are at the symmetry position $(1 - x, -y, 1 - z)$.

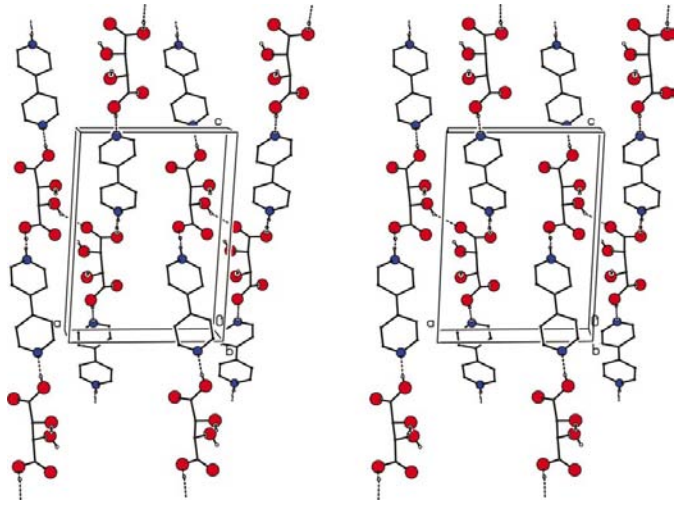

Figure 13
Stereoview of part of the crystal structure of (IV) showing the action of the [021] and [02$\bar{1}$] chains in linking the (100) sheets into bilayers. For the sake of clarity, H atoms bonded to C are omitted.

Despite the similarities in composition and constitution between the salts formed by racemic tartaric acid with piperazine and DABCO, respectively, the corresponding salts formed with these two amines by (2*R*,3*R*)-tartaric acid are entirely different. As already noted, piperazine forms the simple 1:1 salt (V); however, DABCO forms a 3:4 adduct (VIII), whose constitution is that of the salt containing four types of ion $[\{HN(CH_2CH_2)_3NH\}^{2+}]_2\cdot[N(CH_2CH_2)_3NH]^{+}\cdot[(C_4H_5O_6)^{-}]_3\cdot[C_4H_4O_6]^{2-}$. For the sake of convenience and simplicity, we shall discuss first the structure of (V), then that of (VI) and (VII), and finally that of (VIII).

The anion substructure is two-dimensional. In (V) (Fig. 15) both hydroxyl groups act as hydrogen-bond donors, with just one carboxylate atom, O2, acting as the acceptor in the O—H···O hydrogen bonds. Atom O6 in the anion at (x, y, z) acts as a hydrogen-bond donor to O2 in the anion at $(-1+x, y, z)$, thus generating by translation a $C(6)$ chain running parallel to the [100] direction (Fig. 16): likewise O5 at (x, y, z) acts as a donor to O2 at $(2-x, -\frac{1}{2}+y, -z)$, thus producing a $C(5)$ chain running parallel to the [010] direction and generated by the 2_1 screw axis along $(1, y, 0)$. The combination of these two chain motifs generates a (001) sheet in the form of a (4,4) net (Batten & Robson, 1998) built from a single type of $R_4^3(18)$ ring (Fig. 16). A single sheet of this type passes through each unit cell, centred at $z = ca$ 0.25, and adjacent pairs of sheets are linked by the cations to form a three-dimensional pillared-layer framework, in which each cation is linked to four different anions in two different sheets. Atoms N11 and N14 in the cation at (x, y, z) act as hydrogen-bond donors, *via* H11*A* and H14*B*, respectively, to O4 at (x, y, z) and to O3 at $(-1+x, y, z)$ (Table 2), which are both components of the (001) sheet about $z = 0.25$. The same N atoms act as donors, *via* H11*B* and H14*A*, respectively, to O1 at $(x, y, 1+z)$ and to O2 at $(-1+x, y, 1+z)$, both of which lie in the (001) sheet about $z = 1.25$ (Fig. 17). Propagation of these hydrogen bonds by translation generates the continuous three-dimensional structure.

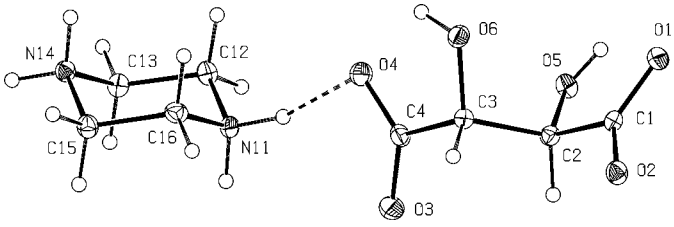

Figure 15
The molecular components of (V) showing the atom-labelling scheme. Displacement ellipsoids are drawn at the 30% probability level.

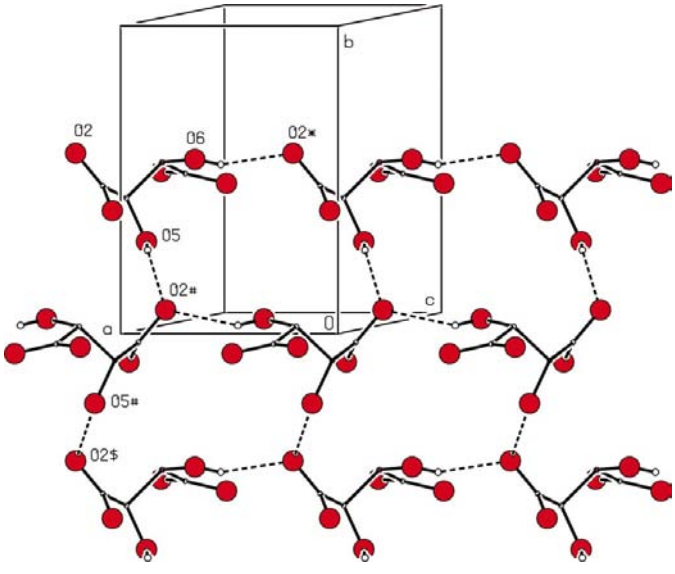

Figure 16
Part of the crystal structure of (V) showing the formation of a (001) sheet built from $R_4^3(18)$ rings. For the sake of clarity, H atoms bonded to C are omitted. The atoms marked with an asterisk (*), hash (#) or dollar sign ($) are at the symmetry positions $(-1+x, y, z)$, $(2-x, -\frac{1}{2}+y, z)$ and $(x, -1+y, z)$, respectively.

The anion substructure is three-dimensional. Although (VI) and (VII) both contain three-dimensional anion frameworks which contain large voids enclosing the cations, there are detailed differences between them, both in the construction of the frameworks and in the cation–anion linkages. This is immediately illustrated by the ionic components (Figs. 18 and 19). In (VI) (Fig. 18) the equatorial N—H bond forms a hydrogen bond with hydroxylic O5, while the axial N—H bond is linked to O3 in the anion at $(1+x, y, z)$. By contrast, in (VII) (Fig. 19) the single N—H bond forms a three-centre hydrogen bond within the asymmetric unit with O3 and O6;

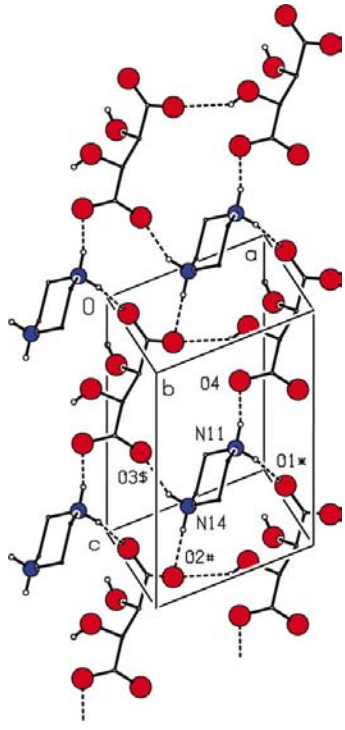

Figure 17
Part of the crystal structure of (V) showing the linking of the (001) sheets by the cations. For the sake of clarity, H atoms bonded to C are omitted. The atoms marked with an asterisk (*), hash (#) or dollar sign ($) are at the symmetry positions $(x, y, 1+z)$, $(-1+x, y, 1+z)$ and $(-1+x, y, z)$, respectively.

however, O5 is not an acceptor of conventional hydrogen bonds, but see below for short C—H···O contacts involving O5.

In (VI) carboxyl O1 in the anion at (x, y, z) acts as a hydrogen-bond donor to carboxylate O3 at $(x, y, -1+z)$, thus generating by translation a $C(7)$ chain running parallel to [001]; hydroxyl O6 at (x, y, z) acts as a donor to carboxylate O4 at $(-\frac{1}{2}+x, \frac{3}{2}-y, -\frac{1}{2}+z)$, thus producing a $C(5)$ chain, running parallel to the [101] direction and generated by the glide plane at $y = 0.75$. The combination of the [100] and [101] chains generates a (010) sheet in the form of a (4,4) net (Batten & Robson, 1998) built from a single type of $R_4^4(22)$ ring (Fig. 20). Two sheets of this type pass through each unit cell, one in the domain $0.55 < y < 0.95$ and the other in the domain $0.05 < y < 0.45$, and these sheets are linked by a further O—H···O hydrogen bond. Hydroxyl O5 in the anion at (x, y, z) is part of the (010) sheet in the domain $0.55 < y < 0.95$: this acts as a hydrogen-bond donor to carboxyl O2 in the anion at $(-x, 1-y, -z)$, which lies in the $0.05 < y < 0.45$ sheet (Fig. 21); similarly, O5 in the anion at $(-\frac{1}{2}+x, \frac{3}{2}-y, -\frac{1}{2}+z)$, which is also a component of the $0.55 < y < 0.95$ sheet, acts as a donor to O2 at $(-\frac{1}{2}-x, \frac{1}{2}+y, -\frac{1}{2}-z)$, which lies in the anion sheet in the domain $1.05 < y < 1.45$. Hence, each (010) sheet is linked by this hydrogen bond to the two adjacent sheets, thereby forming a three-dimensional anion framework. This framework encapsulates large centrosymmetric voids, centred at the origin and the unit-cell centre, whose total volume represent *ca* 24% of the unit-cell volume. The cations lie within these spaces linked to the anion framework by N—H···O hydrogen bonds; as in (V), each cation in (VI) is linked to four different anions (Fig. 21).

The formation of the anion framework in (VII) is rather similar to that in (VI). In (VII) carboxyl O1 at (x, y, z) acts as a hydrogen-bond donor to carboxylate O3 at $(x, y, 1+z)$ and hydroxyl O6 acts as a donor to carboxylate O4 at $(\frac{1}{2}+x, \frac{3}{2}-y, \frac{1}{2}+z)$. Thus, the chain and ring formation is similar to that in (VII), and the resulting (010) anion sheet still lies in the domain $0.55 < y < 0.95$, although the directions of the chains are reversed (*cf.* Figs. 20 and 22). Hydroxyl O5 at (x, y, z), part of the sheet in the domain $0.55 < y < 0.95$, acts as a hydrogen-bond donor to carboxyl O2 at $(-x, 1-y, 2-z)$, part of the sheet in the domain $0.05 < y < 0.45$, thus producing an $R_2^2(10)$ ring (Fig. 23). Again the three-dimensional framework encapsulates voids, in this case representing *ca* 34% of the unit-cell volume.

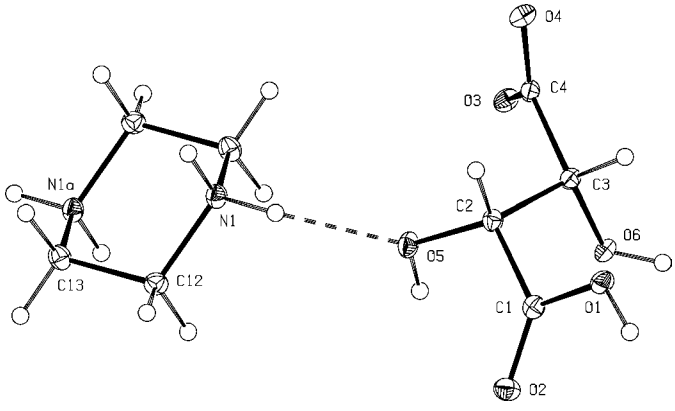

Figure 18
The molecular components of (VI) showing the atom-labelling scheme. Displacement ellipsoids are drawn at the 30% probability level. The atom marked 'a' is at the symmetry position $(1-x, 1-y, 1-z)$.

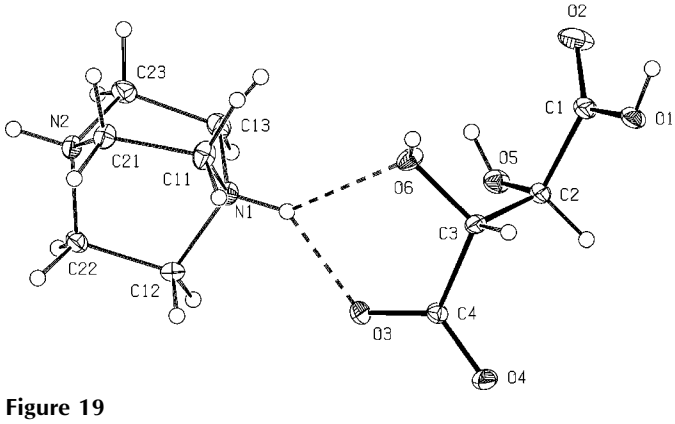

Figure 19
The molecular components of (VII) showing the atom-labelling scheme. Displacement ellipsoids are drawn at the 30% probability level. For the sake of clarity, only one orientation of the DABCO unit is shown.

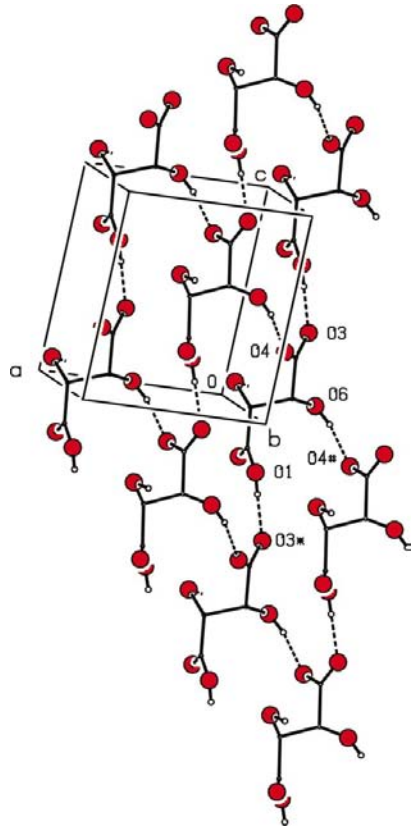

Figure 20
Part of the crystal structure of (VI) showing the formation of a (010) sheet by the anions alone. For the sake of clarity, H atoms bonded to C are omitted. The atoms marked with an asterisk (*) or hash (#) are at the symmetry positions $(x, y, -1+z)$ and $(-\frac{1}{2}+x, \frac{3}{2}-y, -\frac{1}{2}+z)$, respectively.

The linking of the cation to the anion framework in (VII) is complicated somewhat by the orientational disorder of the cations. The cation adopts two orientations across the centre of inversion at $(\frac{1}{2}, \frac{1}{2}, \frac{1}{2})$, each with occupancy 0.5, but the N atoms in these orientations are not coincident (Fig. 24). Atom N1 in the cation at (x, y, z) forms a three-centre hydrogen bond with O3 and O6, also at (x, y, z), while N2 in the same cation forms a similar three-centre system with O3 and O6, both in the anion at $(1 - x, 1 - y, 1 - z)$. Hence, in (VII) each cation is hydrogen-bonded to only two anions, whereas in (VI) each cation is linked to four anions. While in (VII), hydroxyl O5 is not an acceptor of hard hydrogen bonds, as it is in (VI), it nonetheless participates in a rather unusual soft multi-centre C—H···O interaction, whose character is strongly dependent on the structure of the DABCO skeleton. This has approximate D_{3h} symmetry, with the C—H bonds in each $-CH_2CH_2-$ bridge almost fully eclipsed. There are thus four H atoms in a rectangular array on such a bridge and in (VII) atom O5 in the anion at (x, y, z) makes close contacts with the four H atoms bonded to C11 and C21 in the cation at $(-1 + x, y, z$; Fig. 25, Table 2). The C—H···O angles, in the range 351–373 K, are all far too small for these contacts to be regarded as conventional C—H···O hydrogen bonds, although three of the four H···O distances are in the range 2.42–2.55 Å, typical of those in weak C—H···O hydrogen bonds. While this novel non-covalent interaction is possibly adventitious, it certainly suggests that other salts and co-crystals containing DABCO may be worthy of re-examination.

Although the unit-cell dimensions of compounds (VI) and (VII) are similar, as are their general architectures, the differences manifested in Figs. 20 and 22 can be traced to the cation orientations within the respective unit cells. For the reference cations located across the centres of inversion at $(\frac{1}{2}, \frac{1}{2}, \frac{1}{2})$, the (010) projections of the N···N vectors for the two systems are almost orthogonal: hence the locations of the (010) sheets in the cells must differ.

The unusual salt of DABCO and (2*R*,3*R*)-tartaric acid. By comparison with the rather simple salt (VII) formed between DABCO and racemic tartaric acid, the 3:4 stoichiometry of the corresponding product (VIII) formed with (2*R*,3*R*)-tartaric acid is unexpected, as is its constitution $[\{HN(CH_2CH_2)_3NH\}^{2+}]_2 \cdot [N(CH_2CH_2)_3NH]^+ \cdot [(C_4H_5O_6)^-]_3 \cdot [C_4H_4O_6]^{2-}$. The various ionic components (Fig. 26) are linked into a three-dimensional framework by no fewer than 23 hard hydrogen bonds, seven of N—H···O type, one of O—H···N type and 15 of O—H···O type. As usual in multi-component systems, the specification of the asymmetric unit is open to a wide choice: however, in (VIII) it is possible to select a linear, unbranched asymmetric unit in which tartrate units and DABCO units alternate (Fig. 27). All of the N—H···O and O—H···N hydrogen bonds and five of the O—H···O hydrogen bonds lie within the selected asymmetric unit (Table 2), leaving ten O—H···O hydrogen bonds which link these seven-component aggregates into the three-dimensional framework. This framework is readily analysed in terms of

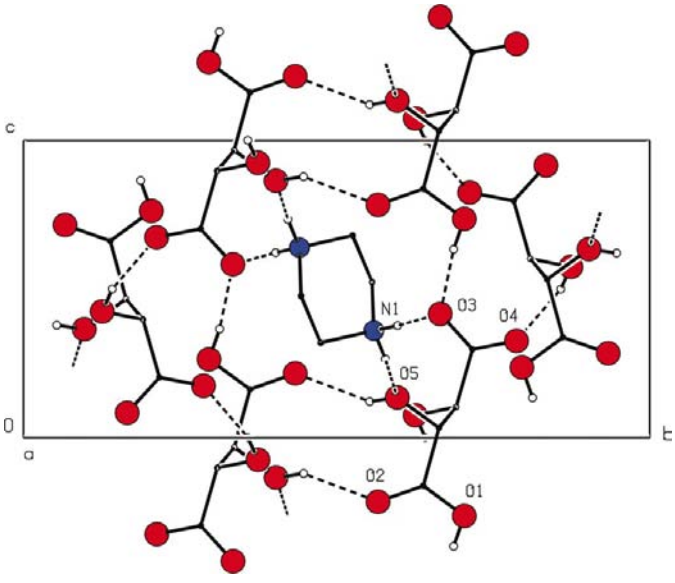

Figure 21
Projection of part of the structure of (VI) showing the linking of the (010) anion sheets by the cations. For the sake of clarity, H atoms bonded to C are omitted.

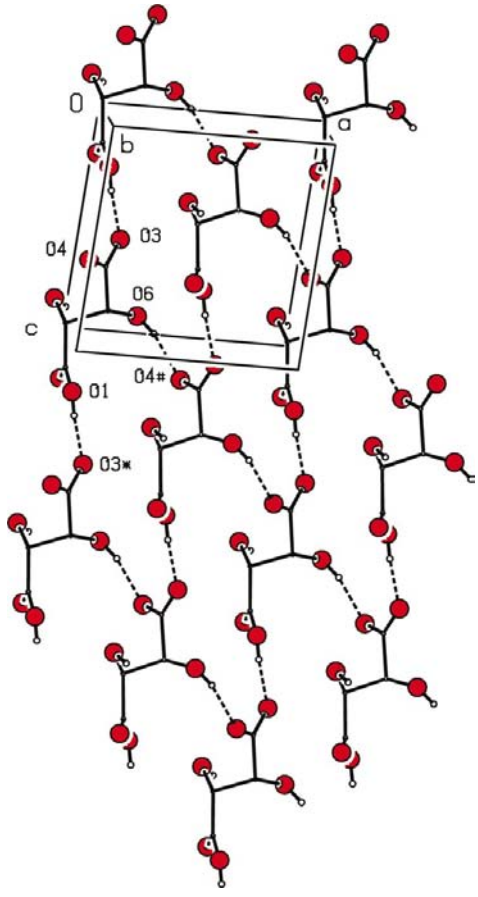

Figure 22
Part of the crystal structure of (VII) showing the formation of a (010) sheet by the anions alone. For the sake of clarity, H atoms bonded to C are omitted. The atoms marked with an asterisk (*) or hash (#) are at the symmetry positions $(x, y, 1 + z)$ and $(\frac{1}{2} + x, \frac{3}{2} - y, \frac{1}{2} + z)$, respectively.

rather simple motifs running parallel to the [100], [010] and [001] directions.

In the [100] direction there are two readily identified substructures: one is a chain of fused rings utilizing just two of the four anions and the other is a molecular ladder involving the other two anions and one of the $[\{HN(CH_2CH_2)_3NH\}^{2+}]$ cations. In the chain of fused rings (Fig. 28), hydroxyls O15 and O16 at (x, y, z) act as hydrogen-bond donors, respectively, to O42 at $(\frac{1}{2}-x, 1-y, -\frac{1}{2}+z)$ and to O41 at $(\frac{3}{2}-x, 1-y, -\frac{1}{2}+z)$, while O45 at $(\frac{1}{2}-x, 1-y, -\frac{1}{2}+z)$ and O46 at $(\frac{3}{2}-x, 1-y, -\frac{1}{2}+z)$ act as donors to O12 and O11, respectively, at (x, y, z). In this way a chain of alternating $R_2^2(10)$ and $R_2^2(12)$ rings is generated running parallel to [100]. In the molecular ladder along [100] (Fig. 29), the uprights are represented by chains of anions in which $(C_4H_5O_6)^-$ and $(C_4H_4O_6)^{2-}$ types alternate and the rungs are represented by one of the cations. Hydroxyls O25 and O35 in the anions at (x, y, z) act as hydrogen-bond donors to carboxylate O32 and O23, respectively, in the anions at $(\frac{1}{2}+x, \frac{3}{2}-y, 1-z)$, while O25 and O35 at $(\frac{1}{2}+x, 1.5-y, 1-z)$ act as donors to O32 and O23 at $(1+x, y, z)$. These interactions generate two equivalent $C_2^2(11)$ chains running parallel to [100]: each pair of anions at a given symmetry position is linked by a cation, thus producing the molecular ladder, between the rungs of which there are $R_6^6(33)$ rings.

The same cation–anion combination which generates the [100] molecular ladder also generates a chain of rings running parallel to [010], simply by the use of a different combination of O—H···O hydrogen bonds to link the anions (Fig. 30). As in the molecular ladder, the fundamental substructure here involves N61 and N62 acting as hydrogen-bond donors to O24 and O34, respectively, and a chain of rings is generated by translation along the [010] direction. Hydroxyl O36 at (x, y, z) acts as a hydrogen-bond donor to O24 at $(x, 1+y, z)$, while hydroxyl O26 at $(x, 1+y, z)$ acts as a donor to O34 at (x, y, z). These interactions thus generate a $C_3^2(12)$ $[R_2^2(10)]$ chain of rings.

These three substructures (Figs. 28–30) utilize eight of the ten interaggregate hydrogen bonds. Each of the two remaining O—H···O hydrogen bonds generates a simple chain motif, which when combined together generate a (100) sheet. In the anion at one extremity of the seven-component aggregate (Fig. 27), carboxyl O14 at (x, y, z) acts as a donor to carboxylate O12 at $(1-x, -\frac{1}{2}+y, \frac{1}{2}-z)$: propagation of this interaction produces a $C(7)$ chain running parallel to the [100] direction and generated by the screw axis along $(\frac{1}{2}, y, \frac{1}{4})$. In a similar manner the anion at the opposite end of the seven-component aggregate gives rise to a second $C(7)$ chain,

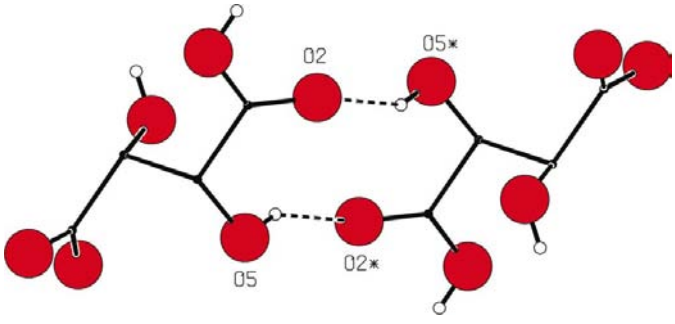

Figure 23
Part of the crystal structure of (VII) showing the $R_2^2(10)$ motif linking components of two (010) anion sheets. For the sake of clarity, H atoms bonded to C are omitted. The atoms marked with an asterisk (*) are at the symmetry position $(-x, 1-y, 2-z)$.

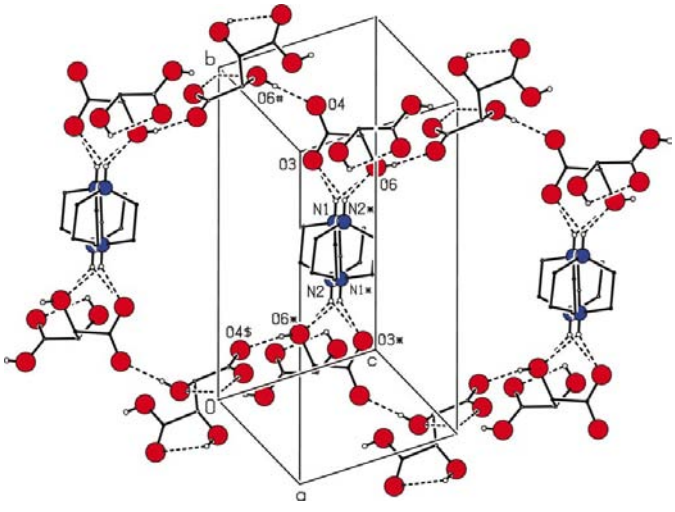

Figure 24
Part of the crystal structure of (VII) showing the linking of the anion sheets by the disordered cations. For the sake of clarity, H atoms bonded to C are omitted. The atoms marked with an asterisk (*), hash (#) or dollar sign ($) are at the symmetry positions $(1-x, 1-y, 1-z)$, $(-\frac{1}{2}+x, \frac{3}{2}-y, -\frac{1}{2}+z)$ and $(\frac{1}{2}-x, -\frac{1}{2}+y, \frac{1}{2}-z)$, respectively.

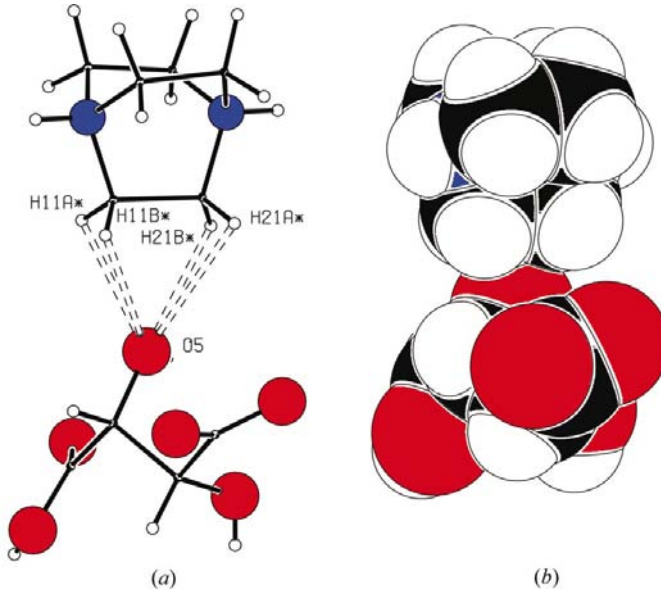

Figure 25
Part of the crystal structure of (VII) showing the very short contacts between O5 and four C—H units on one face of the cation; (*a*) with the C—H···O contacts shown as dotted lines where the atoms marked with an asterisk (*) are at the symmetry position $(-1+x, y, z)$; (*b*) as a space-filling representation.

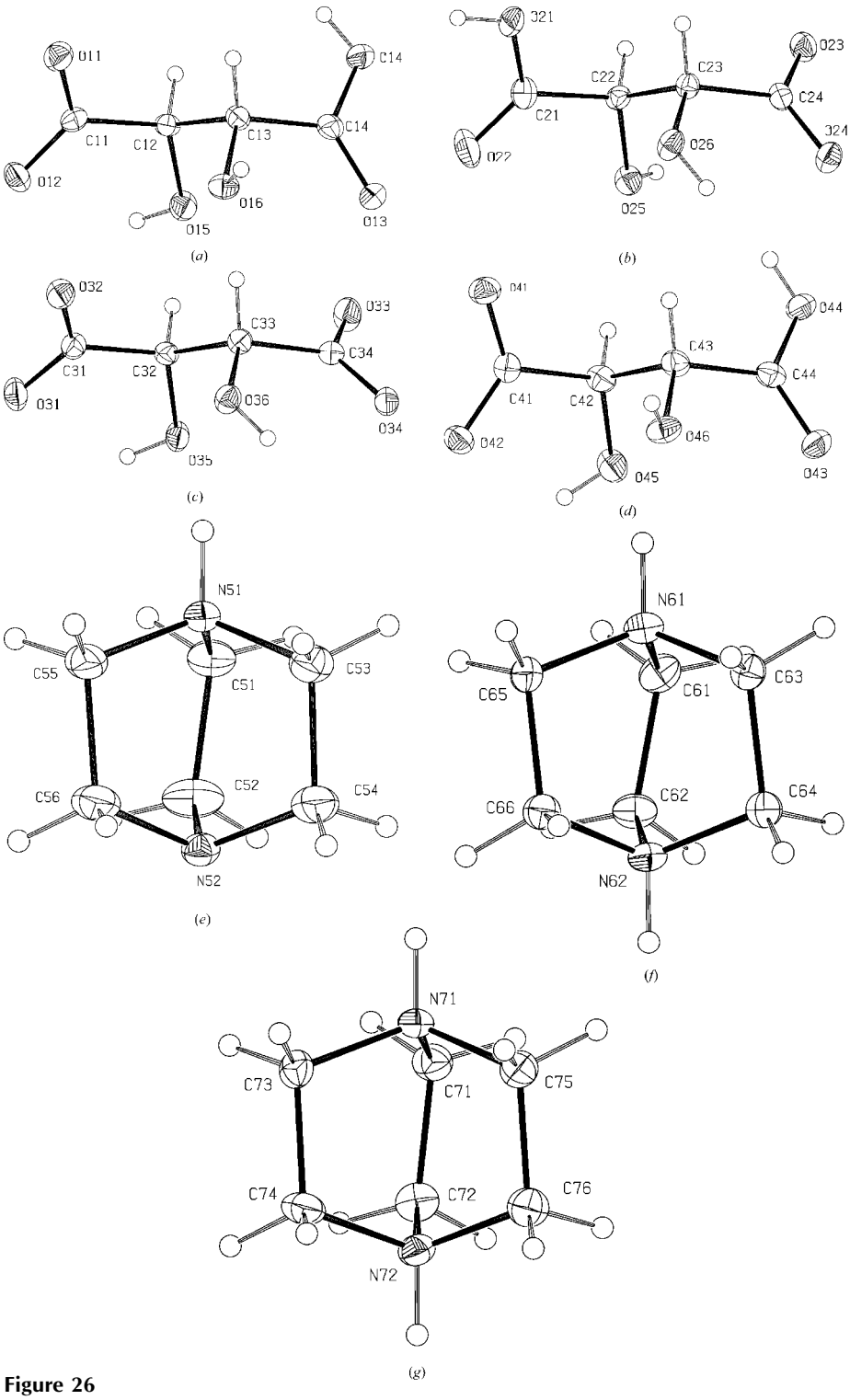

Figure 26
The seven independent molecular components of (VIII) showing the atom-labelling scheme. Displacement ellipsoids are drawn at the 30% probability level.

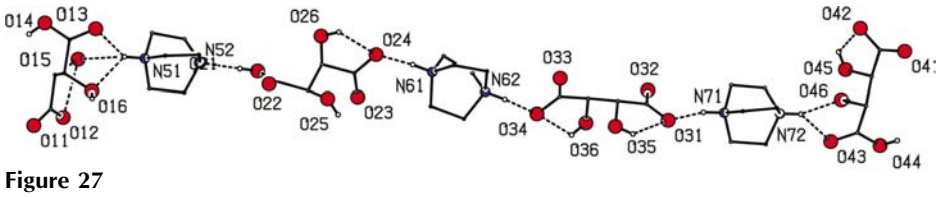

Figure 27
The connected asymmetric unit of (VIII). For the sake of clarity, H atoms bonded to C are omitted.

running antiparallel to the first: O44 at (x, y, z) acts as a donor to O42 at $(1-x, \frac{1}{2}+y, \frac{3}{2}-z)$, generating a chain around the screw axis along $(\frac{1}{2}, y, \frac{3}{4})$. These two $C(7)$ chains are built from the ions at the two ends of the seven-component aggregate and they are thereby linked; their combined effect is to generate a (100) sheet, which is, of course, reinforced by the [010] chain of rings (Fig. 30). The combination of the two [100] motifs (Figs. 28 and 29) with this sheet is sufficient to generate the three-dimensional framework.

3.3. Chirality and pseudosymmetry

For the single-sheet and bilayer structures formed by the bipyridyl species, (I)–(IV), it is striking how similar, in general terms, are the architectures of the chiral and racemic pairs (I)/(II) and (III)/(IV). In the case of (I) and (II), where the space groups are $P\bar{1}$ and $P1$, respectively, (II) mimics space group $P\bar{1}$ with 83% of the non-H atoms conforming to the centrosymmetric space group: the main non-fitting atoms are the carboxyl O atoms of the anions. Compounds (II) and (IV) again exhibit very similar supramolecular architectures, albeit in space groups $P\bar{1}$ and $P2_1$, respectively: as already noted (§3.2.2) the unit-cell vectors of these two compounds are rather similar. In both of these pairs the structures are either centrosymmetric or they closely mimic centrosymmetry.

While (V) and (VI) have different stoichiometries and space groups $P2_1$ and $P2_1/n$, respectively, a 1:2 salt of (2*R*,3*R*)-tartaric acid and piperazine analogous to (VI) has been reported (Aakeröy *et al.*, 1992) to crystallize in space group $P4_12_12$ with a unit-cell volume roughly double that of (VI): again the structure, although non-centrosymmetric, closely mimics centrosymmetry. The two DABCO salts (VII) and (VIII), while exhibiting radically different supramolecular structures, again conform to the general expectation that the different forms of tartaric acid will lead to

different space groups: here the salts crystallize in $P2_1/n$ and $P2_12_12_1$, respectively.

3.4. Hydrogen-bond dimensions

The hydrogen-bond dimensions are listed in Table 2. For (V)–(VIII), where the hard hydrogen bonds generate three-dimensional supramolecular structures, we have not, for the sake of simplicity and brevity, considered any contribution of the soft hydrogen bonds as these can have no effect on the overall dimensionality. The sole exception to this generalization is the rather unusual multi-centre contact discussed above (§3.2.3) for (VII). In (I)–(IV), where the C—H···O hydrogen bonds undoubtedly do influence the overall dimensionality of the supramolecular structures, all of these hydrogen bonds are strong for their type: the H···O and C···O distances lie in the ranges 2.37–2.50 and 3.202 (5)–3.448 (3) Å, respectively, with mean values 2.40 and 3.303 (5) Å, and the C—H···O angles range from 141 to 175° with mean value 157°.

The non-centred N—H···O hydrogen bonds fall naturally into three categories: those involving protonated pyridyl donors; two-centre hydrogen bonds with protonated piperazine and DABCO as donors; and three-centre N—H···$(O)_2$ systems, also with protonated piperazine and DABCO as donors. Those in the first category are all very short with N···O distances in the range 2.478 (4) Å in (IV) to 2.627 (3) Å in (I), with N—H···O angles mostly above 170°. The two-centre N—H···O hydrogen bonds in the piperazine salts (V) and (VI) are unexceptional, but for those in the DABCO systems (VII) and (VIII) there is a very marked difference between the two-centre and the three-centre interactions. The mean values, for the two- and three-centre types, of the H···O and N···O distances are: 1.67 and 2.07, and 2.605 (4) and 2.828 (45) Å, respectively; the corresponding mean values of the N—H···O angles are 167 and 137°. Although the majority

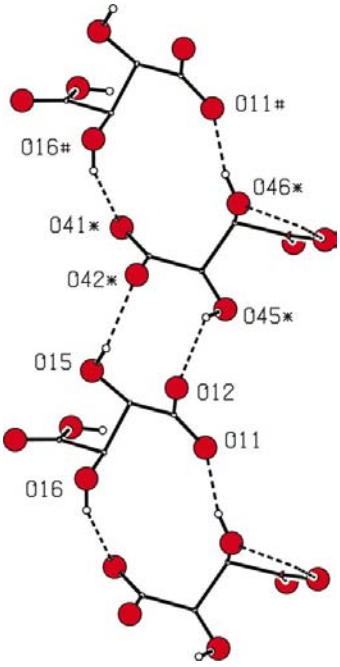

Figure 28
Part of the crystal structure of (VIII) showing the formation of a chain of fused $R_2^2(10)$ and $R_2^2(12)$ rings. For the sake of clarity, H atoms bonded to C are omitted; likewise the unit-cell box is omitted. The atoms marked with an asterisk (*) or hash (#) are at the symmetry positions $(\frac{1}{2}-x, 1-y, -\frac{1}{2}+z)$ and $(-1+x, y, z)$, respectively.

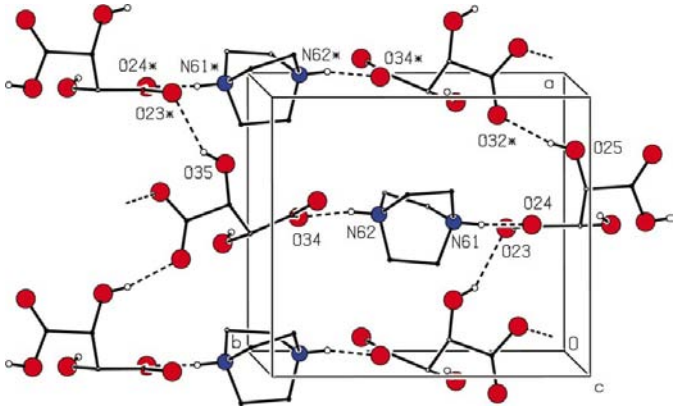

Figure 29
Part of the crystal structure of (VIII) showing the formation of a molecular ladder parallel to [100]. For the sake of clarity, H atoms bonded to C are omitted. The atoms marked with an asterisk (*) are at the symmetry position $(\frac{1}{2}+x, \frac{3}{2}-y, 1-z)$.

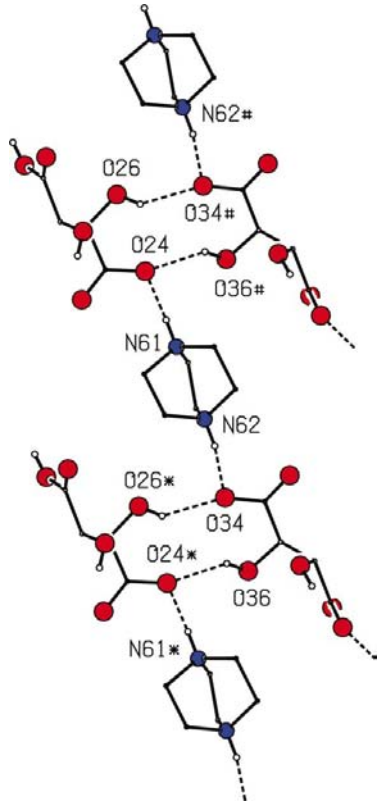

Figure 30
Part of the crystal structure of (VIII) showing the formation of a $C_3^2(12)$ $[R_2^2(10)]$ chain of rings parallel to [010]. For the sake of clarity, H atoms bonded to C are omitted; likewise the unit-cell box is omitted. The atoms marked with an asterisk (*) or hash (#) are at the symmetry positions $(x, 1+y, z)$ and $(x, -1+y, z)$, respectively.

of these hydrogen bonds are components of three-centre systems, the two-centre examples are certainly all short and strong for their type. Likewise, the rather small number of O—H···N hydrogen bonds are all short and strong for their type with the H···N distances in the range 1.67–1.82 Å, the O···N distances in the range 2.479 (4)–2.656 (4) Å and the O—H···N angles in the range 161–178°. As usual in acid–base systems of this general type, N—H···N hydrogen bonds are entirely absent.

Owing to the propensity of the carboxyl groups in tartaric acids to form intramolecular O—H···O hydrogen bonds, many of these bonds are in fact components of three-centre systems. For the two-centre bonds between anions only, the H···O distances range from 1.65 to 2.02 Å (mean value 1.85 Å), the O···O distances from 2.489 (3) to 2.803 (4) Å [mean value 2.666 (4) Å] and the O—H···O angles from 141 to 176° (mean value 166°). Again, the O—H···O hydrogen bonds are in general short and strong for their type. Undoubtedly, the strength of all types of hydrogen bond encountered in this study owes much to the fact that all of the individual molecular components, whether derived from the acid or from the diamine components, have charges enhanced by proton transfer (Aakeröy & Seddon, 1993; Gilli *et al.*, 1994).

4. Concluding comments

The supramolecular structures reported and analysed in this paper indicate clearly that where the chiral and racemic forms of tartaric acid, an exemplar of simple chiral acids, form adducts of common stoichiometry with a given diamine, then the overall supramolecular structures of the two products are remarkably similar despite the different space groups exhibited. Indeed, the structures involving the chiral acid closely mimic centrosymmetry in a number of cases. Against this useful generalization, it is noted that even the product stoichiometries observed here are, in a number of cases, neither predictable nor amenable to simple rationalization, despite the chemical simplicity of the molecular building blocks employed.

X-ray data were collected at the University of Toronto using a Nonius Kappa-CCD diffractometer purchased with funds from NSERC (Canada).

References

Aakeröy, C. B., Hitchcock, P. B. & Seddon, K. R. (1992). *J. Chem. Soc. Chem. Commun.* pp. 553–555.
Aakeröy, C. B. & Seddon, K. R. (1993). *Chem. Soc. Rev.* **22**, 397–407.
Batten, S. R. & Robson, R. (1998). *Angew. Chem. Int. Ed.* **37**, 1460–1494.
Bootsma, G. A. & Schoone, J. C. (1967). *Acta Cryst.* **22**, 522–532.
Braga, D., Grepioni, F., Biradha, K., Pedireddi, V. R. & Desiraju, G. R. (1995). *J. Am. Chem. Soc.* **117**, 3156–3166.
Brock, C. P. & Dunitz, J. D. (1994). *Chem. Mater.* **6**, 1118–1127.
Burchell, C. J., Ferguson, G., Lough, A. J. & Glidewell, C. (2000). *Acta Cryst.* B**56**, 1054–1062.
Burchell, C. J., Ferguson, G., Lough, A. J. & Glidewell, C. (2001). *Acta Cryst.* C**57**, 311–314.
Coupar, P. I., Glidewell, C. & Ferguson, G. (1997). *Acta Cryst.* B**53**, 521–533.
Ferguson, G. (1999). *PRPKAPPA*. University of Guelph, Canada.
Ferguson, G., Coupar, P. I. & Glidewell, C. (1997). *Acta Cryst.* B**53**, 513–520.
Ferguson, G., Glidewell, C., Gregson, R. M. & Meehan, P. R. (1998). *Acta Cryst.* B**54**, 139–150.
Flack, H. D. (1983). *Acta Cryst.* A**39**, 876–881.
Flack, H. D. & Bernardinelli, G. (2000). *J. Appl. Cryst.* **33**, 1143–1148.
Gilli, P., Bertolasi, V., Ferretti, V. & Gilli, G. (1994). *J. Am. Chem. Soc.* **116**, 909–915.
Glidewell, C., Ferguson, G., Gregson, R. M. & Lough, A. J. (1999). *Acta Cryst.* C**55**, 2133–2136.
Lavender, E. S., Ferguson, G. & Glidewell, C. (1999). *Acta Cryst.* C**55**, 430–432.
Nonius (1997). *Kappa-CCD Server Software*, Windows 3.11 Version. Nonius BV, Delft, The Netherlands.
Okaya, Y., Stemple, N. R. & Kay, M. I. (1966). *Acta Cryst.* **21**, 237–243.
Otwinowski, Z. & Minor, W. (1997). *Methods Enzymol.* **276**, 307–326.
Sheldrick, G. M. (1997*a*). *SHELXL*97. University of Göttingen, Germany.
Sheldrick, G. M. (1997*b*). *SHELXS*97. University of Göttingen, Germany.
Spek, A. L. (2001). *PLATON*. University of Utrecht, The Netherlands.
Wilson, A. J. C. (1976). *Acta Cryst.* A**32**, 994–996.